Journal Pre-proof

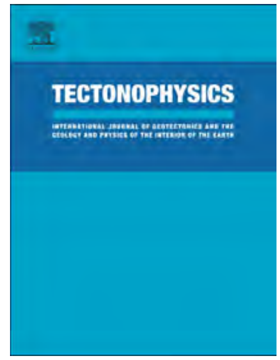

Tectono-stratigraphic evolution of the offshore Apulian Swell, a continental sliver between two converging orogens (Northern Ionian Sea, Central Mediterranean)

Nicolò Chizzini, Andrea Artoni, Luigi Torelli, Jessica Basso, Alina Polonia, Luca Gasperini

PII: S0040-1951(22)00338-9

DOI: https://doi.org/10.1016/j.tecto.2022.229544

Reference: TECTO 229544

To appear in: *Tectonophysics*

Received date: 31 March 2022

Revised date: 28 July 2022

Accepted date: 6 August 2022

Please cite this article as: N. Chizzini, A. Artoni, L. Torelli, et al., Tectono-stratigraphic evolution of the offshore Apulian Swell, a continental sliver between two converging orogens (Northern Ionian Sea, Central Mediterranean), *Tectonophysics* (2022), https://doi.org/10.1016/j.tecto.2022.229544

Tectono-stratigraphic evolution of the offshore Apulian Swell, a continental sliver between two converging orogens (Northern Ionian Sea, Central Mediterranean).

Nicolò Chizzini [1*], Andrea Artoni[1], Luigi Torelli[1], Jessica Basso[1], Alina Polonia[2], Luca Gasperini[2]

1- Department of Chemistry, Life Sciences and Environmental Sustainability University of Parma, Parco Area delle Scienze, 157/A – Parma, Italy

2- Institute of Marine Sciences CNR ISMAR-Bo, Via Gobetti, 101, 40129 Bologna, Italy

Corresponding author: nicolo.chizzini@unipr.it

Keywords: Apulian Swell, Mediterranean Sea; Northern Ionian Sea; Calabrian Arc; Hellenides; transpressive tectonics;

A B S T R A C T

The Calabrian Arc subduction complex, in the northern Ionian Sea, is facing directly the westward subducting Apulian Swell, a sliver of continental crust covered by about 8 km of Mesozoic and Tertiary carbonates. Deformation patterns of this southernmost foreland segment of the Adria plate, analized from marine geological/geophysical data include: 1) flexure/bending, under the load of the advancing Calabrian Arc wedge; 2) buckling in response to compression of the surrounding orogens (southern Apennines, Dinarides-Hellenides); and 3) roll-back and eastward retreat of the slab. In this work, a reprocessed dataset of marine seismic reflection profiles is used to determine the interplay between these tectonic processes during progressive advancement of the Calabrian Arc wedge since Pliocene times. Our analysis indicates that the wedge is presently affected by compressive tectonics along several fore-thrusts, forming an imbricate fan system. Conversely, the Apulian Swell affected by inherited and rift-related Permo-Triassic normal faults, shows transpressive and positive tectonic inversions and, in its southern portion, the effects of the Hellenic fold/thrust belt shortening. The interference between the Calabrian Arc and the Hellenic chain plays an important role in controlling the tectono-stratigraphic evolution of the Apulian Swell, which underwent bending and roll-back during a pre-middle Pliocene stage followed by buckling processes. Active extension observed in the hinge zone of the Apulian Swell between Calabrian Arc and the Hellenides might suggest recent reactivation of flexure and retreat.

1. Introduction

Subduction systems are among the most dynamic geological features of our planet (*Stern, 2002*), and are sites of destructive earthquakes and tsunamis (*Lay, 2015; Bletery, 2016; Wang and Trèhu, 2016*). The Mediterranean area, which includes a network of active and inherited convergent belts, offers a natural laboratory for studying the dynamic processes typical of these geodynamic domains, characterized by subduction and collision processes (*Moretti and Royden, 1988; Royden and Faccenna, 2018*). The Ionian sector of Central Mediterranean (Fig. 1) is an interesting case study, because in a relatively limited area (<150 km) it encompasses a composite suite of subduction-related features, including the overriding Calabrian Arc (CA), with an offshore accretionary wedge as thick as 10 km connecting Sicilian-Maghrebian with the Southern Apennine chain (*Tortorici et al., 1982; Polonia et al., 2011*), the subducting Ionian Lithosphere whose age, origin, and nature are still controversial (*Finetti, 1982; Catalano et al., 2001; Stampfli and Borel, 2002; Hieke* *et al., 2003; Frison de Lamotte et al., 2011; Speranza et al., 2012; Dannowski et al., 2019; Tugend et al., 2019; El-Sharkawy et al., 2021*), and the continental Apulian Swell (AP), the southernmost foreland segment of the Adria Plate (*Handy et al., 2010; Le Breton et al., 2017; Handy et al., 2019; Van Hinsbergen et al., 2020*), overthrusted by the southwest-verging external tectonic units of the Hellenic fold/thrust belt (*Handy et al., 2010; Le Breton et al., 2017; Handy et al., 2019; Van Hinsbergen et al., 2020*) (Fig. 2). To the South of the Kefalonia transfer fault (KTF), the Mediterranean Ridge develops as a Neogene-Quaternary accretionary wedge of the Hellenic subduction zone, where the Hellenic Arc represents the backstop of this convergent system (*Chaumillon and Mascle, 1997; Le Pichon et al., 2002; Kopf et al., 2003; Chamot-Rooke et al., 2005*) (Figs. 1, 2).

The CA and the AP have been subjects of numerous studies highlighting their genesis, architecture, and evolution. The regional geometry of the subduction complex has been described through the analysis of seismological data and seismic reflection profiles (*Rossi and Sartori, 1981; Finetti, 1982; De Voogd et al., 1992; Cernobori et al., 1996; Doglioni et al., 1999; Butler, 2009; Minelli and Faccenna, 2010; Polonia et al., 2011; Volpi et al., 2011; Polonia et al., 2016; Volpi et al., 2017*) and several studies analyzed the structural setting and tectonic evolution of the central and south-western sectors of the CA wedge (*Finetti, 1982; Del Ben et al., 2008; Argnani, 2009; Gallais et al., 2013; Bortoluzzi et al., 2015; Gutscher et al., 2015; Polonia et al., 2016*), as well as its interaction with the AP (*Doglioni et al., 1994; Pieri, 1997; Maesano et al., 2017; Cicala et al., 2021*). However, internal deformation and detailed stratigraphy of the southern Apulian foreland remain not well defined, due to the lacking of exploration wells to calibrate the offshore seismic profiles. This makes the seismo-stratigraphic and structural interpretation of this area a critical issue (*Volpi et al., 2017*). Furthermore, the interaction among the CA wedge, the Hellenic fold/thrust belt, and AP is even less defined. Seismic profiles in the foreland region show active and widespread extensional tectonics (*Doglioni et al., 1999; Argnani, 2006; Del Ben et al., 2010; Argnani et al., 2011; Del Ben et al., 2015; Volpi et al., 2017; Maesano et al., 2020; Cicala et al., 2021*) that is interpreted as the shallow expression of flexural bending induced by the CA and Hellenides tectonic loading on the subducting Apulian slab (*Doglioni et al., 1994; Argnani et al., 2001; Tropeano et al., 2002; Billi and Salvini, 2003; Volpi et al., 2017; Cicala et al., 2021*). However, recent works have also recognized reverse faulting affecting the Apulian foreland that represents a further complexity not explained by available structural models (*Butler, 2009; Del Ben, 2009; Del Ben et al., 2010; Milia et al., 2017; Volpi et al., 2017; Basso et al., 2020*). In this work, we use deep seismic reflection profiles integrated with morphobathymetric data to define the seismo-stratigraphic and structural architecture of the Apulian foreland, the CA wedge, and a portion of the Hellenic fold/thrust belt, with the main purpose of identifing in detail the tectonic processes driving the Late Neogene-Quaternary geological evolution and kinematics of this southernmost portion of the Adria plate.

2. Geological Background

2.1. Tectonic setting and geological evolution

The geodynamic evolution of Central Mediterranean is mainly driven by the N-S Europe/Africa convergence (*Guegen et al., 1998; Faccenna et al., 2001; Carminati & Doglioni, 2005; Polonia et al., 2012; Milia et al., 2017; Jolivet et al., 2021*), that has produced roughly coeval subduction systems of opposing vergence in a complex arrangement (*Moretti and Royden, 1988; Carminati & Doglioni, 2005; Faccenna & Becker, 2010; Mila et al., 2017*). In the Northern Ionian Sea, the westward subduction of the AP beneath the CA is opposite to the eastward directed subduction beneath the Hellenides (*Moretti and Royden, 1988; Minelli & Faccenna, 2010; Polonia et al., 2011; Royden and Papanikolau, 2011; Gallais et al.,* *2012; Polonia et al., 2012; Del Ben et al., 2015; Handy et al., 2019; Volpi et al., 2017*).

2.1.1. The Calabrian Arc wedge

The CA wedge extends mainly in the Ionian offshore and is laterally confined by the Apulia and Malta escarpments (*Argnani & Bonazzi, 2005; Minelli & Faccenna et al., 2010; Polonia et al., 2011; Gallais et al., 2012; Polonia et al., 2012*). In the northern Ionian Sea, the CA and the Apulian foreland are separated by the Taranto Valley, which hosts the submerged part of the Southern Apennine foredeep or the *Bradano Foredeep* (*Senatore et al., 1988; Volpi et al., 2017; Basso et al., 2021*). The CA wedge is a large accretionary complex developed above the southwestward dipping African plate (*Chamot-Rooke et al., 2005; Minelli & Faccenna, 2010; Polonia et al., 2011*), and represents the SE tip of the arcuate Apenninic-Maghrebide fold/thrust belt (*Malinverno and Ryan, 1986; Patacca et al., 1990; Sartori, 1990; Guenguen et al., 1998*). Oblique lithospheric discontinuities separate the CA wedge into two lobes, the *Western* and *Eastern* lobes, that show different structural styles (Fig. 2) (*Polonia et al., 2011; Gallais et al., 2012; Polonia et al., 2016; Bortoluzzi et al., 2017*). They include also two structural domains, i.e., the pre-Messinian and the post-Messinian wedges (*Polonia et al., 2011; Polonia et al., 2016*).

Our study area is entirely located into the Eastern Lobe, and includes the northeastern termination of both pre-Messinian and post-Messinian wedges (Fig. 2). The inner wedge consists of a deformed nappe of pre-Messinian units composed of Tertiary and Mesozoic clastic sediments. Conversely, the post-Messinian wedge is mainly made of Messinian evaporites, overlained by Plio-Quaternary hemipelagites and turbidites (*Polonia et al., 2011; Polonia et al., 2016; Bortoluzzi et al., 2017; Volpi et al., 2017*). The Pliocene-Pleistocene oblique convergence between the Southern Apennines-CA wedge and AP (*Filice &*

Seeber, 2020; Basso et al., 2021) produced an oblique contractional belt (*Ferranti et al., 2014; Volpi et al., 2017*).

2.1.2. The Hellenic Fold/Thrust Belt

The Hellenides are a SW-vergent fold/thrust belt that started to form during Late Jurassic to Early Cretaceous times, with the subduction of Neotethyan Vardar ophiolites subsequetely involved in the collision of the Adria and European Plates around 65 Ma (*Handy et al., 2019*). The collisional belt is formed by allochthnous nappes containing siliciclastic foredeep sediments or "flysch", ranging in age from Late Cretaceous in the NE, to Miocene in the SW, suggesting southwestward propagation of the nappe's stacking (Fig. 3b) (*Schmid et al., 2008; Handy et al., 2019*). In the Tertiary, the Hellenides were affected by the SW-retreating of the eastward subducting AP. A Miocene/Pliocene clockwise rotation of the northern Hellenides (or Albanides) north of the Kefalonia transfer fault zone (*Handy et al., 2019*) was associated to the overall counterclockwise rotation of the Adria Plate (*Le Breton et al., 2017*). Thus, the Hellenides result to be segmented by two major transfer fault zones, i.e., the Othoni-Dhermi Transfer Fault Zone and the Kefalonia Transfer Zone of *Handy et al., (2019*). The latter, according to *Royden and Papanikolau (2011*), is a transform fault that during the Neogene transferred the front of the Hellenides as far as the Mediterranean Ridge (*Kopf et al., 2003*) which faces the Ionian Abyssal Plain and the CA wedge (Fig. 2).

2.1.3. The Apulian Swell (AP)

The foreland region between the opposite-verging CA wedge and Hellenides chain is represented by the southern portion of the Apulian Swell (Fig. 2), which was involved in the Ionian rifting during the Permian-Middle Triassic time, and led to the creation of the Ionian lithosphere before the opening of the Neotethys

(*Vai, 1994; Finetti and Del Ben, 2005; Stampfli, 2005; Del Ben et al., 2010; Del Ben et al., 2015; Handy et al., 2010*). This extensional phase produced a thick Paleozoic-Triassic sedimentary cover above the crystalline basement (*Patacca et al., 2008*). Since the upper Triassic, a regional shallow water domain has determined the deposition of a thick carbonate platform, that was later fragmented (*Mattavelli et al., 1991; Del Ben et al., 2010; Del Ben et al., 2015*). Starting from early Cretaceous, the Hellenic orogen has moved gradually onto the Apulian foreland (*Channel et al., 1979; Del Ben et al., 2015*) causing the transition between carbonate to siliciclastic sedimentation (*Del Ben et al., 2015*); at the same time, thrusting within the internal parts of the Hellenides involved both sedimentary rocks and their crystalline basement (*Moretti and Royden, 1988*). The clastic turbidites, originated from the Southern Apennine-CA and Dinaric-Hellenic orogens, reached the AP and the Adriatic basin to the north only during Oligocene-Early Miocene times (*Mattavelli et al., 1991*) and filled the Bradano and the Hellenic foredeeps.

The Neogene evolution of Southernmost Adria Plate is considered the result of slab rollback of both, the Ionian and Hellenic slabs, driving shortening and accretion coeval with back arc extension in the forearc of both Tyrrhenian Sea (*Malinverno and Ryan, 1986; Jolivet and Faccenna, 2000; Faccenna et al., 2001; Sartori, 2003*) and the internal zone of the Hellenides (exhumation of the Pelagonian units and Rhodope Massif, *Papanikolau, 2003; Royden and Papanikolau, 2011; Burg et al., 2012*) and Aegean Sea (*Carminati & Doglioni, 2005; Jolivet et al., 2021*).

In the Lower Pliocene, the Apulian foreland was affected by flexural bending due to loading of progressively advancing Southern Apennine/CA (*Moretti and Royden, 1988; Argnani et al., 2001; Critelli et al, 2017; Volpi et al., 2017; Critelli, 2018; Maesano et al., 2020; Cicala et al., 2021*). This phase triggered extension and formation of NW-SE normal faults (*Ciaranfi et al., 1988; Argnani et al., 2001;*

Finetti & Del Ben, 2005; Del Ben et al., 2010; Volpi et al., 2017; Cicala et al., 2021) and the deep and narrow Bradano foredeep basin (Fig. 2) at the toe of the frontal thrust belt (*Casnedi, 1988; Butler, 2009; Volpi et al., 2017*), filled by turbidite sediments (*Moretti and Royden, 1988; Rossi et al., 1988; Artoni et al., 2019; Basso et al., 2021*). In the early Pliocene, up to early Pleistocene, the Southern Apennines-CA nappes overthrusted the Apulian foreland, which underwent a compressional phase (*Mostardini and Merlini, 1986; Del Ben et al., 2015; Basso et al., 2021*). During the Middle Pleistocene, the CA started rotating clockwise onto and along the old passive margin of the Apulian carbonate platform (*Del Ben et al., 2008*), causing oblique convergence (*Basso et al., 2021*). Resisting subduction, this foreland forced the chain to decelerate and changing direction from ESE-ward to SSE-ward (*Van Dijk and Scheepers, 1995; Del Ben et al., 2008; Del Ben et al., 2010; Del Ben et al., 2015*).

At the eastern edge, slab rollback produced forward movement of the Hellenic arc towards the continental lithosphere of the AP (*McKenzie, 1978; Le Pichon and Angelier, 1979; Finetti, 1982; Jackson & McKenzie, 1988; Moretti and Royden, 1988; Finetti et al., 1991; de Voogd et al., 1992; Finetti & Del Ben, 2005; Del Ben et al., 2015*) and the oceanic lithosphere of the Sirte abyssal plain (Fig. 2). Therefore, our study area represents a crucial region to better understand both deep and shallow subduction processes that affected the AP; the effects of these processes are recorded in the Apulian foreland which is the foreland of both CA wedge and Hellenic orogen, respectively related to the westward and eastward directed subduction of the AP.

2.2. Stratigraphy of the Apulian Swell

The continental AP, that shows a flat Moho discontinuity at 28-32 km depth (*Amato et al., 2014*), is mainly made of (Fig. 3a): 1) Upper Triassic dolomitic and evaporitic sediments resting unconformably on the Lower Triassic-Permian terrigenous deposits, corresponding to the sedimentary cover of the crystalline basement (*Ricchetti et al., 1988; Patacca et al., 2008; Del Ben et al., 2010; Volpi et al., 2017; Maesano et al., 2020*); 2) 4-7 km thick Mesozoic carbonates (*Nicolai & Gamberini, 2007; Mila et al., 2017*), constituted of Cretaceous limestones and Jurassic dolostones that laterally pass to pelagic sequences in intra platform basins (*Nicolai and Gambini, 2007; Del Ben et al., 2015*); 3) Miocene open-ramp carbonate deposits, followed by Messinian evaporites that locally disconformably cover the Jurassic-Cretaceous carbonates (*Catalano et al., 2001; Patacca et al., 2008; Del Ben et al., 2010*); 4) the Plio-Quaternary deposits consist of clastic turbidites (marl and clay sediments) (*Rossi et al., 1983; Rossi and Borsetti, 1984; Del Ben et al., 2010; Minelli and Faccenna, 2010; Volpi et al., 2017; Maesano et al, 2020*) with the lower portion represented by the early Pliocene rhythmically bedded pelagic deposits of the Trubi Formation (*Cita & Gartner, 1973; Rossi & Borsetti, 1974; Volpi et al., 2017; Maesano et al., 2020*) and late Pliocene to early Pleistocene coarse-grained, bioclastic cool-water carbonate (*Tropeano et al., 2022*). Based on the analysis of offshore data, a stratigraphic scheme of the Plio-Pleistocene sedimentary succession for the Apulian foreland has been recently proposed (*Basso et al., 2021)*; this scheme is based on the three regional-unconformities that extend those defined by *Zecchin et al.* (*2015*) in the CA and nearshore CA wedge (Fig. 3c): 1) Pliocene unconformity (PCU); 2) mid-Pliocene (MPCU); 3) early Pleistocene (EPSU); and 4) mid-Pleistocene (MPSU). These unconformities record episodes of tectonic uplift associated with contractional-transpressive events that interrupted longer phases of subsidence associated with high accumulation rates (*Zecchin et al., 2015; Basso et al., 2021*). This led to infer a cyclic pattern of Plio-Pleistocene subsidence and uplift (P1-P4 cycles) in which unconformities record the interference between the Adria Plate and the adjacent orogens during pauses in subduction retreat (Fig. 3c) (*Ferranti et al., 2014; Basso et al., 2021; Cicala et al., 2021*). These regional unconformities can be recognized in the study area as major unconformities bounding the seismo-stratigraphic units (see § 4); in particular, the PCU corresponds and/or merges to the Messinian Unconformity, the MPCU corresponds to top of lower Pliocene unit, and the EPSU and the MPSU are inside the Upper Pliocene to Holocene unit. These unconformities locally merge/converge or diverge depending on the differential basin's subsidence or uplift and consequent number of stratigraphic hiatuses. However, they can be traced both into the Bradano Foredeep and CA wedge, toward West, and into the Hellenic foredeep and Hellenides, toward East (Fig. 3 and see § 4).

3. Material and methods

A group of selected multichannel seismic reflection (MCS) profiles were analysed and interpreted to reconstruct the seismo-stratigraphic sequences and structures of the CA wedge, as well the adjacent Apulian foreland (Fig. 4). Four among 80 MCS profiles, for a total length of 3000 km in an area of 22.963 km^2 (Fig. 4) were selected (acquisition parametrers and technical specification are shown in Tab.1). *Line-1* and *-2* were kindly provided by ENI SpA, while *Lines-3* and *-4* were acquired by the CROP Project during the 90's, and are publicly available at *http://www.crop.cnr.it/*. Due to the lacking of wells, particular attention was paid to analyze seismo-acoustic characters of reflectors, including amplitude, frequency and continuity, that allowed to define the seismic *facies* and the limits of depositional sequences (*Vail et al., 1987; Sukumono & Ambarsari, 2019; Al-Masgari et al., 2021*).

The MCS dataset was integrated by morphobatimetric data provided by EMODnet Bathymetry Consortium (2020) available at *https://www.seadatanet.org/*, which host high-resolution data (1/16 x 1/16 arc minutes - ~100 m in the deep sea). Data were analyzed and displayed using the Global Mapper v. 21 software (*http://www.bluemarblegeo.com/*) and artwork with the software Adobe Illustrator®.

4. Results and interpretations

4.1 Seismic stratigraphy and structural interpretation

Interpretation of the selected multichannel seismic profiles enable us to describe the seismo-stratigraphic units, as well as the seismic *facies* and the main tectonic elements in the different domains in the study region (Figs. 5-9).

4.1 Apulian foreland and Bradano-Hellenic foredeep basins

4.1.1 Plio-Quaternary seismic sequences

The Plio-Quaternary deposits consist of Upper Plio-Holocene and the Lower Pliocene sequences separated by an unconformity defined as MPCU in the literature (Figs. 3c-(2), 5a) (*Zecchin et al., 2015; Volpi et al., 2017; Basso et al., 2021*). The thickness of the Upper Plio-Holocene sediments is variable from 0.250 to 0.150 s TWT, reaching a maximum (1 s TWT) in the Bradano and Hellenic foredeep basins. Here, the Upper Plio-Holocene package sediments, marked by sub-parallel and continuous reflectors, onlap the apulian monocline, with terminations younger in the Bradano and the Hellenic foredeeps, to the East and the West, respectively (Figs. 6f, 9a, 9b). Two major unconformities have been recognized in the Upper Plio-Holocene sequence, and correlated with the EPSU and the MPSU in agreement with previous works in the Bradano Foredeep (*Zecchin et al., 2015; Basso et al., 2021*) (Fig. 6f) and the Hellenic Foredeeep (Fig. 9a, 9b). The two unconformities EPSU and MPSU merges in the central portion of AP where the youngest is considered to be present and the amount of stratigraphic hiatus is hard to define precisely (Figs. 6a,c,d, 7,8). In the NNE sector the Apulian foreland is characterized by an irregular and rugged topography, as shown in Figs. 6c and in bathymetric profile 1 (Fig. 10), indicating active or recently inactivated submarine erosion. Below the Upper Plio-Holocene sequence, a semi-transparent seismic unit has been correlated to Lower Pliocene deposits, in agreement with *Volpi et al.* (*2017*). This unit (0.2 to

0.35 s TWT) is marked by medium frequency/low-amplitude, semi-trasparent, sub-parallel and continuous reflectors (Fig. 5a).

Beneath the Bradano foredeep, the Lower Pliocene sediments rest conformably on the Messinian evaporites while they are accreted in the allochtonous units within the advancing CA wedge (Fig. 6e, 6f). The irregular seafloor of the Apulian foreland suggests active or recently inactivated tectonic deformations (Fig. 11). In fact, the ESE sector is characterized by the presence of extensional tectonics, evidenced by high-angle, EW-dipping normal faults, which cut off the Lower Pliocene but they are sealed by the Upper Plio-Holocene deposits (Fig. 6c). This indicates that most faults are no longer active, except for a few extensional deformations affecting the Holocene sediments and the seafloor, where they are associated with morphological scarps at the seafloor (Fig. 7b).

At the intersection between Line-1 and Line-2, the seafloor appears widely dislocated by two NNE and SSW dipping normal faults, producing a prominent horst structure named HS, and controlling the formation of two basins, i.e., the Northern Basin (NB) and the Southern Basin (SB), also described in *Maesano et al.*(*2020*) (bathymetric map and profile 4 in Fig. 10; Figs. 6c, 7c). These two prominent faults and the sourronding normal faults belong to an extensional NW-SE oriented faults system in the foreland, the SAFS (South Apulia Fault System; *Maesano et al., 2020*). Along the NE dipping normal fault bounding the HS horst, pre-Messinian and Plio-Quaternary sediments are brought in contact by the fault (Figs. 6c, 7c). Here, the Upper Pliocene-Holocene seismic sequence consists of two syn-tectonic wedges separated by an unconformity, interpreted as the MPSU: an uppermost wide growth wedge (0,150 s TWT) and a lowermost thicker, localized and wedge onlapping toward both NNE and SSW (0,2 s TWT) (Fig. 7d).

However, the foreland region close to the Bradano foredeep is affected by folding processes that involve recent sediments and produce seafloor bulges (Fig. 6d). This might indicate an ongoing compressive/transpressive phase overprinting older normal faults. Positive inversion process has led to uplift and back-rotation of the normal fault's hanging walls, producing gentle bulges of the Upper Plio-Holocene sediments (B1, B2, B3, Fig. 6d). These bulges are also visible in the bathymetric Profile 3 (Fig. 10). Inversions generated also back-thrusts and narrow pop-up structures cutting across the shallow sediments (Fig. 6d).

Moving to the ESE area and nearby the Hellenic fold/thrust belt, the Plio-Quaternary deposits are crosscut by a set of high-angle opposite dipping reverse fault splaying out into positive flower structures, which testify transpressional tectonics (Fig. 11). Two positive flower structures, named PF2 and PF3, affect the Lower Pliocene sediments (Figs. 8, 9a, 9b) and are associated in their uppermost part to shallower reverse faults, cutting the semi-transparent Lower Pliocene seismic sequence (Fig. 9b). These positive structures are sealed by relatively undeformed Upper Plio-Holocene Hellenic foredeep sediments, suggesting that these two flower structures are no longer active (Fig. 9b). Instead, moving to the South, the Plio-Quaternary deposits sealing the carbonate platform are folded and they create a wide uplift visible on the bathymetry (Profile 5 in Fig. 10). Here, the Upper Plio-Holocene seismo-stratigraphic unit is folded and six narrow positive flower structures affect the seabed (PF4 to PF9 in Fig. 10; see also the bathymetric Profile 5 in Fig. 10) and suggest active or recent compressive/transpressive tectonics. Seafloor bulges are probably linked to positive inversion tectonics and they agree with the recent (Middle-Upper Pleistocene) compressive-transpressive regime recognized by *Del Ben et al.* (*2010*).

4.1.2 Pre-Pliocene seismic sequences: the Messinian event and the Apulian carbonate platform (Jurassic / Cretaceous-Upper Miocene)

The base of the Lower Pliocene unit is marked by a prominent high-amplitude continuous reflector, constituting the top of the Messinian unit, the so called Messinian unconformity (Fig. 5a) (*Doglioni et al., 1999; Merlini et al., 2000; Butler, 2009; Volpi et al., 2017; Maesano et al., 2020*). This relatively thin Messinian unit (0.1 to 0.08 s TWT) appears layered with continuos reflectors (Fig. 5a), which loose coherence towards the foredeep basins. In the SE and E foreland area, as shown in Seismic Line 3 and Seismic Line 4 (Figs. 8, 9a), the Messinian unconformity separates Plio-Quaternary sediments and platform carbonates. Here, the Messinian deposits appear to be missing, probably due to their very limited thickness, lower than the seismic resolution. As mentioned above, the Plio-Quaternary and the Messinian units overlay a carbonate platform sequence through a strong reflector (Fig. 5a), which represents the top of the Cretaceous-Upper Miocene carbonates of the Apulian platform.

The underlaying Cretaceous-Upper Miocene carbonate platform sequence of the Apulian Mesozoic-Tertiary platform is 1.0 to 0.6 s TWT and it is characterized by seismic *facies* made of sub parallel high-amplitude reflectors (Fig. 5a, b). The boundary with the underlying seismic sequence, correlated with Jurassic carbonates, is constituted by a major unconformity with onlap terminations (Mesozoic unconformity in Fig. 5b) and, below the foredeep basin, by a sharp truncation (Fig. 6f). The Jurassic sequence (2.0 to 2.6 s TWT) includes two different seismic *facies* (Fig. 5b): 1) a well layered unit with sub-parallel continuous reflectors and high-moderate amplitudes, interpreted as related to intra-platform basinal deposits; and 2) a massive seismic *facies* interpreted as marking reefal carbonate platform deposits. Underneath the Messinian unconformity, both the Jurassic and the Cretaceous-Upper Miocene seismic sequences show discontinuous reflectors, particularly in the SSW sector and in the NNE foreland investigated by Seismic Line 2 (Figs. 5c, 7b). Here, the Jurassic carbonate platform shows a chaotic/blind seismic *facies* (1 s TWT), where seismic signal is almost wiped-out (Fig. 5c).

Seismic interpretations show that the Apulian carbonate platform and the Messinian unit are affected both by extensional and compressive/transpressive tectonics. NNE and SSW active dipping normal faults generally affect these pre-Pliocene sequences (Figs. 6c, 7b). As shown in Seismic Line 2, in the NNE foreland sector both the Cretaceous-upper Miocene and the Jurassic units appear folded and associated with the antiformal structures named A1, A2, A3, A4, suggesting a compressive tectonics stage (Figs. 7a, 7e). These antiformal structures are cut by the extensional faults and sealed by the Upper Plio-Holocene sequence (Fig. 7e). In the HS interpreted in Seismic Line 1-2 (Figs. 6c, 7c) the Cretaceous-Upper Miocene and Jurassic reflectors seem also largely folded and disrupted, due to the presence of a positive flower structure (PF1; Figs. 6c, 7c, 11) which was either lately dismembered or is undergoing dismemberment by the extensional tectonics. In the southermost Hellenic sector, the Mesozoic carbonate platform reflections look also largely folded and associated to the positive flower structures PF2 to PF9 bounded by faults striking NE-SW (Figs. 8, 11). These positive flower structures are widespread in the southern Apulian foreland where they are grouped into the AITZ (Adriatic-Ionian Transpressive Zone) (Fig. 11).

4.1.3 Upper Triassic/Lower Triassic-Upper Permian seismic sequences

The base of the Jurassic sequence has been located at a prominent high-amplitude reflector (Figs. 5c, d). According to the literature, this underlying seismic sequence corresponds to the Upper Triassic carbonate platform (*Del Ben et al., 2009; Del Ben et al., 2010; Del Ben et al., 2015; Volpi et al., 2017*) and shows moderate amplitude/frequency sub-parallel reflectors (Figs. 5c, 5d). It is bounded at the base by a high-amplitude reflection which probably corresponds to the top of the Lower Triassic-Upper Permian sequence, tentatively assigned to the sedimentary cover of the crystalline basement, as also defined by previous works (Fig. 5d) (*Patacca et al., 2008; Del Ben et al., 2010; Maesano et al., 2020*). These deepest seismic sequences are affected by a widespread extensional tectonics highlighted by several NNW-SSE dipping normal faults, defining Triassic rifted basins, in some cases sealed by the overlying Jurassic platform (Figs. 6a, 7a, 7e) as interpreted by many authors (*Doglioni et al., 1994; Merlini et al., 2000; Stampfli, 2005; Patacca et al., 2008; Del Ben et al., 2010; Basso et al., 2021*). This first ritfing phase has been linked to the beginning of the break-up of Pangea that started since Early Permian to Late Triassic (*Dewey et al., 1973; Dewey et al., 1989; Garcìa-Mondejar et al., 1989; Bertolotti et al., 1993; Calvet et al., 1993; Frizon de Lamotte et al., 2000; Lòpez-Gòmez et al., 2002; Calvet et al., 2004; Stampfli, 2005; Handy et al., 2010; Frizon de Lamotte et al., 2011*).

4.2 The Calabrian Accretionary Wedge

The prism's seafloor shows a very irregular morphology, especially in the internal western sector of the domain, characterized by depressions interpreted as submarine canyons originated by erosional processes. Here, a wedge-top basin (WB) associated with shallow normal faults is imaged (Fig. 6b; Profile 1 in Fig. 10). In this domain, the Upper Plio-Holocene sequence (0,2 to 0,7 s TWT) is characterized by sub-parallel reflectors above a major unconformity which has been attributed to the MPSU that, toward East, merge with EPSU and MPCU and it can be correlated within the entire study area (Figs. 6b-e). Both Upper Plio-Holocene unit and underlaying lower Pliocene seismic sequences (0.3 to 0.8 s TWT) show divergent reflections configuration testifying syn-tectonic sedimentation (Fig. 6b). The Upper Pliocene-Holocene package onlaps the lower Pliocene unit, as observed in Fig. 6b. Beneath lower Pliocene unit and at the top of a chaotic allochthonus assemblage of accreted Jurassic-Upper Miocene sediments, a seismic *facies* shows a clear stratification with discontinuous high-amplitude reflections (Figs. 6b, 6e); this seismic characters are clearly distinguishable from the surrounding ones and are attributed to the Messinian unit (0,3 to 0,4 s TWT) but no well constraints this age.

The CA wedge is mainly caracterized by compressive tectonics. Its front is marked by eastward verging thrusts, forming a leading imbricate fan system overriding deposits of the narrow Bradano foredeep basin (Figs. 6e, 11). Here, the Plio-Quaternary foredeep sediments gently dip towards the prism, are crosscut by the sole thrust and onlap the flexed AP. In the innermost CA wedge sector, the Messinian and the Plio-Quaternary seismic sequences show evidence of internal folding due to compressive tectonics generated by a complex system of E and W verging thrusts and backthrusts, whose association constitutes pop-up structures and triangle zones (Figs. 6e, 11). Positive inversion processes seems also to involve the subducted AP and the bottom of the chaotic assemblage, probably due to the ongoing and active migration of the CA toward the Ionian domain, here evidenced by five Subducted Inverted Faults (SIF): four E-verging high-angle reverse faults (SIF1, SIF2, SIF4, SIF5) and one W-verging high-angle reverse fault (SIF3) affect the subducted carbonate platform and the sole thrust of the accretionary prism, resulting in gentle folding of the latter (Figs. 6e, 11).

4.3 Hellenides external deformation front

In the eastermost sector of the study area, the AP is inclined toward the Hellenic foredeep basin, and it seems to be involved and accreted into the Hellenic deformation front (Fig. 9a). Even if this tectonic domain is not analyzed in detail in this work, it is clearly characterized by compressional structures reaching the seafloor, mainly W verging thrusts which costituite an imbricate fan system as already defined by many authors (*Aubouin et al., 1970; Aubouin et al., 1976; Kamberis et al., 1992; Kamberis et al., 1996; Kamberis et al., 1998; Kilias et al.,* *2001; Le Pichon et al., 2002; Zelilidis et al., 2003; Marnelis et al., 2007; Mila et al., 2017; Kamberis et al., 2021).* This imbricate system is delimited by a blind thrust in its W external sector that is sealed by the Upper Plio-Holocene deposits of Hellenic foredeep; anyway, the Upper Plio-Holocene sequence is also deformed by the more internal fronts of the Hellinides. The Oligocene foredeep turbiditic deposits and the Neogene Molasse with deltaic deposits of the Sazani zone (Fig. 3b) (*Zelilidis et al., 2003; Zelilidis et al., 2015; Kamberis et al, 2021*) are also part of the Hellenides, while their distal, basinward portions are included in the Cretaceous-upper Miocene unit and Plio-Quaternary deposits of the Apulian foreland (Figs. 3b, 9b).

5. Discussion

The selected seismic reflection profiles encompass the eastern part of the CA wedge and the Apulian foreland, including the western front of the Hellenides. The analyses of seismic data allow us reveal the complex tectono-stratigraphic evolution of this area (e.g., *Doglioni et al., 1999; Merlini et al., 2000; Argnani, 2001; Nicolai and Gambini, 2007; Butler, 2009; Del Ben et al., 2009; Del Ben et al., 2010; Mila et al., 2017; Volpi et al., 2017; Basso et al., 2021; Cicala et al., 2021*). It also outlines recent tectonic processes, enphasizing the role of the opposite verging and advancing CA and Hellenides in controlling the offshore Apulian foreland architecture and stratigraphy.

5.1 Tectono-stratigraphic evolution

Although the geodynamic setting of Central Mediterranean is dominated by the N-S plate convergence, the Apulian Swell should be part of a relatively stable crustal block trapped between two deforming chains. However, seismic data show that the foreland is affected by both compressive/transpressive and extensional tectonic deformation. Since the Triassic, shallow-water marine deposits formed the Mesozoic-Tertiary Apulian carbonate platform, made of a succession of massive reef carbonates and pelagic sediment (Fig. 5b), as already observed in the Apulia foreland domain by many authors (*Nicolai and Gambini, 2007; Del Ben et al., 2010; Del Ben et al., 2015; Volpi et al., 2017*). Our seismic interpretation supports that the Jurassic platform was affected by extensional faulting, thus defining an important Jurassic rifting phase (Figs. 12a, 13a). This event caused fragmentation of the existing platform in a series of carbonate blocks (*Nicolai & Gambini, 2007*) bounded by extensional faults that appear to strike both NNE-SSW and SSE-NNW (Fig. 12a). Seismic data also show that an important erosive event affected the Apulian platform, as highlighted by a clear unconformity, i.e., the Mesozoic unconformity, corresponding to the Jurassic-Cretaceous carbonate boundary (Figs. 5b, 13a), probably caused by emergence of wide platform sectors during sealevel lowstand. This led to the Jurassic platform dismantling and the consequent formation of an irregular and rugged morphology at its top, and formation of bauxite surfaces (*Bosellini et al., 1993*). The overlaying Cretaceous-Upper Miocene carbonate platform deposits and the shallow water sediments appear also affected by extensional tectonics (Figs. 12a, 13a1). The Hellenides folds, that initatied to develop by this time to the East (*Handy et al., 2019*), created foredeep basin here included in the Cretaceous-Upper Miocene unit (Fig. 13a1).

The end of Mesozoic-Tertiary Apulian foreland tectono-stratigraphic evolution is marked by the Messinian dissecation of the Mediterranean basins, occurred 5.97-5.33 Ma (*Krijgsman et al., 1999; Manzi et al., 2020; Pellen et al., 2022*). The foreland ramp was unconformably overlained by the Messinian evaporitic sediments, attributed to the thin layered unit above the Cretaceous-Upper Miocene sequence (Fig. 13b). The irregular loss of signal in the seismic image within the carbonate platform (Fig. 7b) is interpreted as the result of the Messinian relative sea-level low stand in the Mediterranean, that favored emersion of large parts of the platform partly karstified (*Butler, 2009*) and affected by erosion. The widespread emersion is also evidenced by a clear regional unconformity (the Messinian unconformity) followed by an extensional regime in the foreland and re-activation of previous Mesozoic faults (Figs. 12b, 13b). The Messinian erosion is also recorded in the advancing CA wedge and the Hellenides where compression was active. In the CA wedge an important Messinian compressive tectonic phase is highlighted by the Messinian Unconformity on the top of the chaotic assemblage and Messinian evaporites being part of the allochthonous units (*Polonia et al., 2011; Zecchin et al., 2015; Basso et al., 2021*). The latter contains Cretaceous platform-to-basin limestone and Miocene foredeep deposits (*Casero et al., 1988; Merlini et al., 2000; Patacca & Scandone, 2007; Van Dijk et al, 2011; Basso et al., 2021*) testifying that collision and the CA wedge were already present (*Facenna et al., 2010; Vitale & Ciarcia et al., 2013*) and the Apulian foreland was experiencing an initial flexuration (Fig. 13b). At the same time, the Hellenic sector was also affected by a compressive tectonic phase and formation of the Messinian unconformity (*Kamberis et al., 1996; Kamberis et al., 2000; Kamberis et al., 2020*). Above the Messinian Unconformity, the semi-transparent seismic sequence identified in both domains (Apulian foreland and CA wedge) has been attribuited to the pelagic deposits of the Lower Pliocene Trubi Formation, in agreement with previous works (*Volpi et al., 2017; Maesano et al., 2020*). This unit indicates that, starting from the Lower Pliocene, the Apulian Swell was drowned and returned to submarine conditions (*Benson, 1973; Cita & Ryan, 1973; Cita, 1975; Cita et al., 1990; Rouchy et al., 2001; Roveri et al., 2014; Sciuto & Baldanza, 2020; Pellen et al., 2022*). At the same time, extensional tectonic continued to affect the Apulian foreland (Fig. 13b), witnessed by the presence of Lower Pliocene syn-tectonic wedge interpreted in seismic data (Figs. 6c, 13b).

Afterward, the wedges of CA-Southern Apennines and Hellenides thrusted over the Lower Pliocene deposits covering the Apulian carbonate platform (*Mostardini & Merlini, 1986; Catalano et al., 2004; Mila et al., 2017*), leading to a compressive stage in different zone of the Apulian foreland (Figs. 12c, 13c); in the case of Southern Apennines, the translation is several tens of km (*Casero et al., 1988; Merlini et al., 2000; Basso et al., 2021*). This compressive stage, recorded by the regional Middle Pliocene angular unconformity (MPCU) and Early Pleistocene angular unconformity (EPSU) (*Zecchin et al., 2015; Volpi et al., 2017; Zecchin et al., 2020*; *Basso et al., 2021*), is related to the genesis of positive flower structures (PF1 to PF9, Figs. 6c, 7c, 8, 9; see also the structural map, Fig. 11) and antiformal structures A1 to A4 (Figs. 7a, 7e) described in this work. We interpreted these compressive structures as generated by opposite verging reverse faults, enucleated along inherited normal faults linked to the previous Mesozoic extensional phase and then inverted. At the same time, previous Messinian-Early Pliocene extensional faults associated to the bulge of the flexed Apula plate, are also replaced by compressive tectonics *(Del Ben et al., 2009; Del Ben et al., 2010*). Foreland inversion in the study area and in the Taranto Gulf were proposed by previous studies (*Merlini et al., 2000*; *Butler, 2009*; *Basso et al., 2021*). Moreover, coeval compressive structures were also identified in the eastern sector of the foreland nearby the Hellenides (*Milia et al., 2017*). Seismic data confirm the existence of these compressive structures and we propose that the progressive advancement of the CA wedge and Hellenides led to the transmission of compressive stresses to the Apulian foreland from opposite directions, resulting in the reactivation of early normal faults as reverse faults while the gentle folding of the carbonate platform and Lower Pliocene sediments generated antiformal structures (A1 to A4; Figs. 7a, 7e) and the nine positive flower structures described in this study (PF1 to PF9). We consider this positive inversion phase limited to the Middle Pliocene/pre-MPSU because the positive flower structures (PF2 and PF3) in the Hellenic foredeep (Figs. 9b) and the antiformal structures (A1 to A4) (Figs. 7a, 7c) are either sealed by the Upper Pliocene-Holocene unfolded sediments or locally crosscut by normal fault such as the dismembered positive flower structure PF1 forming the HS (Figs. 6c, 7c, 11). *Maesano et al*. (*2020*) proposes that the HS is part of an active NW-SE striking extensional faults system, the SAFS, whose location, size and tectonic activity suggests that they could represent a plausible candidate for the source of the 20 Febraury 1743 earthquake occurred in the Northern Ionian Sea (*Maesano et al., 2020;* see also the recent seismicity in Italy*: Rovida et al., 2006; ISIDe Working Group, 2007; Locati et al., 2016*). Our seismic interpretation confirm the remarkable evidence of this recent tectonic activity on the foreland epitomized by the SAFS, also testified by a syn-tectonic extensional wedge in the uppermost portion (post-MPSU) of the Upper Pliocene-Holocene seismic sequence located beside the HS (Fig. 7d). However, inside the HS footwall, the MPCU and especially the reflectors of the Mesozoic sequences are largely positively folded (Fig. 7c). To explain this peculiar geometry, we have hypothesized that a previous transpressive tectonic phase generated the positive flower structure (PF1; Figs. 6c, 7c, 11). This hypothesis can be supported also by the presence of the narrow, lowermost portion of the Upper Pliocene-Holocene sequence beside the HS, corresponding to a post-MPCU and pre-MPSU syn-tectonic wedge (Fig. 7d), which shows the typical characters of a strike-slip basin, similar to the Dagg Basin along the South Alpine Fault zone in New Zealand (*Barnes et al., 2001, 2005*). Unlike syn-tectonic extensional basins, that generally show wide growth wedges thinning away from the fault plane and diverging-thickening strata toward the fault plane (*Allen P.A & Allen J.R., 1990*), basins associated with strike-slip deformation are more complex compared to the latters. In fact, they are generally small and narrow, they form in areas of net shortening (folded Mesozoic reflectors) and are characterized by a rapid spatial evolution with voluminous sedimentation supply and they show syntectonic growth wedges thinning toward the fault (*Allen P.A & Allen J.R., 1990; Barnes et al., 2001*). In our case study, this strike slip basin developed and evolved rapidly during the deposition of lowermost portion of the Upper Pliocene-Holocene sequence (post-MPCU and pre-MPSU) due to the tectonic activity of PF1 against which the sedimentary growth wedge is thinning (Fig. 7d). Then, the PF1 was dismembered by the recent SAFS extensional activity, also witnessed by the uppermost portion of the Upper Pliocene-Holocene (post-MPSU) associated to the NE dipping normal fault bounding the HS (Fig. 7d) as already shown in *Maesano et al.* (2020).

However, since Middle Pleistocene (post-MPSU), another compressional phase is locally testified by folds and positive flower structures affecting the seafloor and deforming the Upper Pliocene-Holocene seismo-stratigraphic unit. The folds SIF1-5 (Figs. 6e, 11, 13d) in the dipping subducted foreland monocline are attributed to this youger compressive phase. They are likely due to the stress transmitted by the CA wedge. Nonetheless, *Butler* (*2009*) proposes that the folds shown in the subducted AP and underneath the CA wedge might be seismic artifact due to pull up velocity because of the higher seismic velocities within the orogenic wedge in comparison with the adjacent foredeep sediments. On the contrary, *Volpi et al.* (*2017*) and *Basso et al.* (*2021*) remark that a tectonic origin of these folds cannot be excluded althought pull-up velocity can modify the geometry of these deeper structures (Transpressed Apulia Block of *Volpi et al., 2017*). The lack of wells and an accurate seismic interval velocities does not allow us to certify the pull-up nature of these folds, so we have interpreted them as originated by inversion tectonics process affecting older Apulian normal fault (SIF1 to SIF5). Compressional structrures affecting the AP are also the gentle and positive bulges (B1, B2, B3) of shallow Upper Plio-Holocene sediments shown in the Seismic Line 1 nearby the Bradano foredeep basin (Fig. 6d and bathymetric Profile 3 in Fig. 10). These gentle anticlines are also attributable to the post-MPSU compressive phase likely associated to the stresses that also shape the CA wedge. Then, in the southern sector of the study area, the re-activation of some of the positive flower structures related to the previous Middle Pliocene compressional phase (specifically PF4, PF5, PF6, PF8, PF9)

(Figs. 8, 11) testify also the occurrence of post-MPSU compression. It is worth to remark that these positive flower structures constitute the NE-SW transpressive zone AITZ (Adriatic-Ionian Transpressive Zone) (Figs. 11, 12c) which parallels the fault system segmenting the Hellenides; namely the Othoni-Dhermi transfer fault and the Kefalonia transfer zone of *Handy et al.* (*2019*) or Kefalonia transform fault of *Royden & Papanikolau* (*2011*). These two fault systems cutting the Hellenides are likely inherited from Mesozoic rifting suggesting that the Adriatic-Ionian Transpressive Zone (AITZ) is also likely related to positive inversion tectonics of Mesozoic structural features that have a polyphased and very likely recent deformation history.

The post-MPSU compressive phase is not widespread or it does not affect the whole Apulian foreland. In fact, in its central part, around the hinge of the AP, extensional faults exist, emphasized by the SAFS mentioned before. The SAFS was activated between 1.3 and 1.8 Ma (*Maesano et al., 2020*) and they are still active, creating morphobathymetric scarps (Figs. 11, 13d) (*Volpi et al, 2017; Maesano et al., 2020*). This observation sets and important constraint as it indicates that, in this sector, normal faults post-date the earlier compressional tectonic stage (post-MPCU and pre-MPSU) and they might be coeval to compressional structures belonging to the AITZ (PF4-PF9), to the SIF1-5 and to the B1-B3 (Fig. 11).

The more recent (post-MPSU) compressional phase can be framed into the oblique and diachronous collision between the CA wedge and the rigid carbonate Apulian foreland that produced a re-orientation of the CA wedge motion. The Apulian foreland, which is resistant to subduction, forced the chain to decelerate and the wedge changed its migration toward SE, inducing a tectonic re-organitation since this age (*Del Ben et al., 2008; Del Ben, 2009; Del Ben et al., 2010; Del Ben et al., 2015; Volpi et al., 2017; Basso et al., 2021*). The CA and the opposite compression from the Hellenides transmitted the stress regime to the AP, causing the reactivation of reverse faults and inversion of inherited extensional faults. Thus, the Middle Pleistocene-Holocene stage (i.e. post-MPSU) poses doubts on the real extent and distribution of the compressional and extensional features in the Apulian foreland, which is either about to being involved in the accretion process of the orogenic wedge or locally behaving as a forebulge area (undergoing extension) after a compressional/transpressional phase that sharply imprint the entire AP from the CA wedge to the Hellenides.

5.2 Mechanisms controlling the extensional and positive inversion tectonics in the Apulian foreland

Extensional tectonics in the Apulian foreland may be explained by flexural bending on the subducted Apulian block induced by the advancing Calabrian/Apennine and Hellenic chains (Fig. 14a, 14b) (*Argnani et al., 2001; Calamita et al., 2003; Argnani et al., 2006; Del Ben et al., 2010; Volpi et al., 2017; Maesano et al., 2020; Sabbatino et al., 2020; Cicala et al., 2021*), likely reactivating older Mesozoic normal faults. Another mechanism that could explain extensional features is the slab rollback (*Malinverno and Ryan, 1986; Patacca et al., 1990; Faccenna et al., 2001; Ferranti et al., 2014*). Rapid rollback of the Ionian and southern Adriatic sectors of AP are thought to have occurred during Miocene-Pliocene, while, during the Quaternary, slab retreat slowed down in the Apennines and Calabria, but not in Southeastern Hellenides (*Faccenna et al., 2001; Serpelloni et al., 2005; Serpelloni et al., 2007; D'Agostino et al., 2008; Ferranti et al., 2014*).

The AP bulge (black arrow in Profile 1, Fig. 10) represents a classical tectonic plate bending (*Sabbatino et al., 2020*), and suggests that flexure is probably the major process controlling the Apulian foreland extensional regime. Spatial correlation between the maximum flexural curvature of the Apulian foreland and development of graben structures indicates a link between the two (*Argnani et al., 2001*). We find and confirm that extensional tectonics coincides with maximun foreland curvature (Fig. 14a), suggesting that extension is roughly coeval with plate flexure certaninly since Lower Pliocene. This low radius flexure could be responsible for moderate seismicity observed in this area (*Argnani et al., 2001*). Extensional faults were subsequently inverted (Fig. 14c) but, at the same time, the flexural extension process continued to produce extension, representing, in some cases, the last tectonic phase in the foreland. This is the reason because of extensions post-dates the compressive/transpressive tectonics, as witnessed by several NE-SW dipping high angle normal faults observed in the seismic lines and associated with prominent escarpment and horst/graben structures such as those belonging to the SAFS (*Maesano et al.*, 2020). These structures are also visible in the bathymetric data, such as the active extensional faults related to the HS structure (Figs. 6c, 7c) and by recent Upper Plio-Holocene (post-MPSU) syn-tectonic wedges, as well as extensional faults cutting the sealed antiformal structures (A1 to A4 in Line 2, Figs. 7a, 7e). However, compressive structures either sealed by the Upper Plio-Holocene sequence or affecting the seafloor are visible close to the CA wedge front (B1-3), the Hellenides (PF2-3 are sealed and PF4-PF9 deforming seafloor), and they are inverted faults in the subducted AP (SIF1-4) (Fig. 11). The genesis of these folds, associated with inverted faults nearby the orogenic front and in the subducted foreland may be related to lithospheric buckling (Fig. 14c) and maximum horizontal stress field (*Cloetingh et al.*, *1999*; *Calamita et al.*, *2003*). Based on our interpretation, this process might be active throughout the Pliocene-Holocene, when the Apulian foreland was affected by compressions as far as the hinge/bulge region. The change of CA wedge tectonic movement from ENE to SE-ward since the Middle Pleistocene (post-MPSU) (*Del Ben, 2009; Del Ben et al., 2008; Del Ben et al., 2010*) may have contributed to the formation of the AITZ transpressive system as well as other compressive structures (Fig. 15); the oblique convergence might have favored a strike-slip component transmitted to the foreland which triggered transpressive tectonics (Fig. 15). In fact, since the Middle Pleistocene tangential forces transmitted by the two opposite advancing wedges to the thick Apulian foreland are recorded by the onset of a strike-slip regime overprinted by a compressive components leading to the observed transpressive deformations (Fig. 15). However, NE-SW dipping normal faults cutting the positive flower structures belonging to AITZ (Fig. 11) suggest that also flexure is again (locally) active in more recent times (since Middle Pleistocene or post-MPSU). The different phases of flexure, buckling and buckling with flexure are related to the complex and time-variable interplay between the advancing CA wedge and Hellenides over the rigid Apulian foreland block which is not a simple flexed and subducting continental sliver.

6. Conclusions

The interaction between the Apulian Swell and the opposite verging Calabrian/Hellenides orogenic wedges has produced a complex tectono-stratigraphic evolution since the Late Miocene.

Seismic data show that structural development in the AP is characterized by different phases and/or coexistence of extensional and compressive/transpressive tectonics, induced by slab rollback, flexural bending, and buckling process.

The advancement of the Calabrian and Hellenic wedges transmitted compressive stress to the foreland, leading to a tectonic inversion of previous Mesozoic and Messinian-Early Pliocene faults since the Middle Pliocene. Changes in the direction of movement of the CA Wedge, associated with oblique convergence, have driven transpressional tectonics that is locally followed by extensional tectonics after Middle Pleistocene (post-MPSU).

The widespread compressive deformation at the contact zone between the AP and the CA wedge suggests that in this sector the west-dipping AP is already incorporated in the orogenic wedge.

However, compressive tectonics, recognized also by the literature and traceable with the seismo-stratigraphic units, is widespread and active in the central sector of the foreland, very far from the two opposite orogenic fronts, implying that collisional tectonics can be propagated over long distances from plate boundaries producing significant deformations ahead of the orogens.

This work suggests that the Apulian Swell cannot be considered a simple subducting continental sliver extended by flexural bending, but it preserves record of repeated late Neogene-Quaternary extensional and compressional pulses.

Acknowledgments

The work is part of the PhD project of N. Chizzini funded by University of Parma – Fondazione Cariparma 2020. We greatly acknowledge ENI S.p.A (A. Fattorini, and C. Cattaneo in particular) for allowing access to seismic reflection database and providing permission to publish seismic images in the frame of the established confidentiality agreement. We are grateful to the Editor R. Carbonell as well as A. Del Ben and an anonymous reviewer for very constructive comments. We are also grateful to F. E. Maesano and L. Ferranti for useful discussions during various meetings, which have help improving this work.

Declaration of interests

The authors declare the following financial interests/personal relationships which may be considered as potential competing interests:

Chizzini Nicolo reports financial support was provided by University of Parma.

References

- Allen P.A, Allen J.R. (1990), *Basin Analysis, Principles & Application*, Blackwell Scientific Publication,115-126.

- Al-Masgari A.A., Elsaadany M., Abdul Latiff A.H., Siddiqui N.A., Hermana M., Imran Q.S., Babikir I., Adeleke T.O. (2021), *A guideline for seismic sequence stratigraphy interpretation*, ARPN Journal of Engineering and Applied Sciences, 16, 2.

- Amato A., Bianchi I., Agostinetti N.P. (2014), *Apulian crust: Top to bottom,* Journal of Geodynamics. DOI: 10.1016/j.jog.2014.09.007.

- Argnani A., Bortoluzzi G., Favali P., Frugoni F., Gasperini M., Ligi M., Marani M., Mattietti G., Mele G. (1994), *Foreland tectonics in the southern Adriatic Sea*, Mem. Soc. Geol. It., 48, 573-578, 4 ff.
- Argnani A., Bonazzi C., Evangelisti D., Favali P., Frugoni F., Gasperini M., Ligi M., Marani M., Mele G. (1996), *Tettonica dell'Adriatico meridionale*, Mem. Soc. Geol. It., 51, 227-237, 10ff.
- Argnani A., Frugoni F., Cosi R., Ligi M., Favalli P. (2001), *Tectonics and seismicity of the Apulian Ridge south of Salento peninsula (Southern Italy)*, Annali di Geofisica, 44, N.3. DOI: 10.4401/ag-3573.
- Argnani A. and Bonazzi C. (2005), *Malta Escarpment fault zone offshore eastern Sicily: Plio-Quaternary tectonic evolution based on new multi-channel seismic data*, Tectonics, 24 (4). DOI: 10.1029/2004TC001656.
- Argnani A. (2009), *Evolution of the Tyrrhenian slab tear and active tectonics along the western edge of the Tyrrhenian subducted slab*, Geological Society of London, Special Publication, 311(1), 193-212. DOI: 10.1144/SP311.7.
- Artoni A., Polonia A., Carlini M., Torelli L., Mussoni P., Gasperini L. (2019), *Mass transport deposits and geo-hazard assessment in the Bradano foredeep (southern Apennines, Ionian Sea)*, Mar. Geol. 407, 275–298. DOI: https://doi.org/10.1016/j. margeo.2018.11.008 .
- Aubouin J., Blanchet R., Cadet J.P., Celet P., Charvet J., Chorowicz J., Cousin M., Rampoux J.P. (1970), *Essai sur la geologie des Dinarides.* Bulletin De La Societe Geologique De France, 12, 1060–1095.
- Aubouin J. (1973), *Des tectoniques superposees et de leur signification par rapport aux modeles geophysiques: L'exemple des Dinarides; paleotectonique, tectonique, tarditectonique*, Bulletin De La Societe Geologique De France, 15, 426-460.
- Aubouin J., Bonneau M., Davidson J., Leboulenger P., Matesco S. (1976), *Esquisse structurale de l'arc Egeen externe: des Dinarides aux Taurides*, Bulletin de la Societe geologique de France 7, XVIII, 327–336.
- Basso J., Artoni A., Torelli L., Polonia A., Carlini M., Gasperini L., Mussoni P. (2021), *Oblique plate collision and orogenic translation of the Southern Apennines revealed by post-Messinian interregional unconformities in the Bradano Basin (Ionian Sea – Central Mediterranean)*, Marine and Petroleum Geology, 128, 104999. DOI: 10.1016/j.marpetgeo.2021.104999.
- Benson R.H. (1973), *Psychrospheric and continental Ostracoda from ancient sediments in the floor of the Mediterranean*. In: Ryan W.B.F., Hsu K.J, Cita M.B., Dumitrica P., Lort J.M., Maync W., Nesteroff W.D., Pautot G., Stradner H. and Weze F.C., *Initial Reports of the Deep Sea Drilling Project*, Washington D.C., vol. XIII, part 1, 1002-1008. DOI: 10.2973/dsdp.proc.13.136-2.1973.
- Bertotti G., Picotti V., Bernoulli D., Castellarin A. (1993), *From rifting to drifting: tectonic evolution of the South-Alpine upper crust from the Triassic to the Early Cretaceous*, Sedimentary Geology 86, 53–76. DOI: 10.1016/0037-0738(93)90133-P.
- Billi A. and Salvini F. (2003), *Development of systematic joints in response to flexure-related fibre stress in flexed foreland plates: the Apulian forebulge case history*, *Italy*, Journal of Geodynamics, 36, 532-536. DOI: 10.1016/S0264-3707(03)00086-3.

- Bletery Q. (2016), *Mega-earthquakes rupture flat megathrust*, Science, 354, 1027-1031. DOI: 10.1126/science.aag0482.
- Bortoluzzi G., Polonia A., Torelli L., Artoni A., Carlini M., Carone S., Carrara G., Cuffaro M., Del Bianco F., D'Oriano F., Ferrante V., Gasperini L., Ivaldi R., Laterra A., Ligi M., Locritani M., Muccini F., Mussoni P., Priore F., Riminucci F., Romano S., Stanghellini G. (2017), *Styles and rates of deformation in the frontal accretionary wedge of the Calabrian Arc (Ionian Sea): controls exerted by the structure of the lower African plate*, Italian Journal of Geoscience, 136, 3, 347-364. DOI: 10.3301/IJG.2016.11.
- Bosellini A., Neri C., Luciani V. (1993), *Platform margin collapses and sequence stratigraphic organization of carbonate slopes: Cretaceous–Eocene, Gargano Promontory, southern Italy, 5(3), 282–297.* DOI: 10.1111/j.1365-3121.1993.tb00259.x.
- Burchfiel B.C. (1980), *Eastern European Alpine system and the Carpathian orocline as an example of collision tectonics*, Tectonophysics, 63, 31-61. DOI: 10.1016/0040-1951(80)90106-7.
- Burg J.P. (2012), *Rhodope: From mesozoic convergence to cenozoic extension. Review of petro-structural data in the geochronological framework*, J. Virtual Explor, 42. DOI: 10.3809/jvirtex.2011.00270.
- Butler (2009), *Relationship between the Apennine thrust belt, foredeep and foreland revealed by marine seismic data, offshore Calabria*, Italian Journal of Geoscience, 128, (2), 269-278. DOI: 10.3301/IJG.2009.128.2.269.
- Calamita F., Paltrinieri W., Pelorosso M., Scisciani V., Tavarnelli E. (2003), *Inherited mesozoic architecture of the Adria continental palaeomargin in the neogene central apennines orogenic system*, Italy, Bollettino Società Geologica Italiana, 122, 307-318, 11 ff.
- Calvet C., Anglada E., Salvany J.M. (2004) *El Triásico de los Pirineos*. In: Vera JA (ed) Geología de España, SGE-IGME, Madrid, p 272–274.
- Calvet F., Solé de Porta N., Salvany J.M. (1993), *Cronoestratigrafía (Palinología) del Triásico sudpirenaico y del Pirineo Vasco-Cantábrico*, Acta Geológica Hispánica, 28: 33–48.
- Carminati E., Doglioni C., (2005), *Mediterranean Geodynamics: Encyclopedia of Geology*, Elsevier, 135–146.
- Casero P, Roure F., Endignoux L., Moretti I., Müller C., Sage L., Vially R. (1988), *Neogene geodynamic evolution of the southern Apennines,* Mem. Soc. Geol. It., 41, 109-120, 3 ff., 3 tavv.
- Casnedi R. (1988), *La fossa bradanica: origine, sedimentazione e migrazione*, Mem. Soc. Geol. It, 4, 439-448, 7ff.
- Capozzi R., Artoni A., Torelli L., Lorenzini S., Oppo D., Mussoni P., Polonia A. (2012), *Neogene to Quaternary tectonics and mud diapirism in theGulf of Squillace (Crotone-Spartivento Basin, Calabrian Arc, Italy)*, Marine and Petroleum Geology, 35, 219–234. DOI: 10.1016/j.marpetgeo.2012.01.007.
- Catalano R., Doglioni C., Merlini S. (2001), *On the mesozoic ionian basin*, Geophys. J. Int., 144, 49–64. DOI: 10.1046/j.0956-540X.2000.01287.x.
- Catalano S., Monaco C., Tortorici L. (2004), *Neogene-Quaternary tectonic evolution of the southern Apennines*, Tectonics, 23, 1-19. DOI: 10.1029/2003TC001512
- Cernobori L. et al (1996), *Crustal image of the Ionian basin and its Calabrian margins, Tectonophysics*, 264, 175-189. DOI: 10.1016/S0040-1951(96)00125-4.
- Chamot-Rooke N., Rangin C., Le Pichon X., Working Group, D.O.T.M.E.D. (2005), DOTMED—*Deep Offshore Tectonics of the Mediterranean: a synthesis of deep marine data in eastern Mediterranean,* [CD-ROM], Mem. Soc. Geol. Fr., 177, 64.
- Channel J.E.T., D'Argenio B., Horvàth F. (1979), *Adria, the African promontory, in Mesozoic Mediterranean paleogeography*, Earth-Sci. Rev. 15, 213–292. DOI: 10.1016/0012-8252(79)90083-7.

- Ciaranfi N., Pieri P., Ricchetti G. (1988), *Note alla Carta Geologica delle Murge e del Salento (Puglia centromeridionale)*, Memorie della Società Geologica Italiana, 41, 449–460.
- Cicala M., Fets V., Sabato L., Tropeano M., Doglioni C. (2021), *Interference between Apennines and Hellenides foreland basins around the Apulian swell (Italy and Greece)*, Marine and Petroleum Geology, 133 (special issue,1):105300. DOI: 10.1016/j.marpetgeo.2021.105300.
- Cita M.B., Gartner M. (1973), *Studi sul Pliocene e gli strati di passaggio dal Miocene al Pliocene*, Riv. Ital. Paleontol. Stratigr., 79, 503e558.
- Cita M.B. & Ryan W.B.F. (1973), *47.5 Time-scale and general synthesis*. *In*: Ryan W.B.F., HSU K.J, Cita M.B., DumitricaP., Lort J.M., Maync W., Nesteroff W.D., Pautot G., Stradner H. and Weze F.C.- *Initial Reports of the Deep Sea Drilling Project*, Washington D.C., vol. XIII, part 1, 1405-1415.
- Cita M. (1975), *Foraminiferal biozonation of Pliocene deep-sea sediments from the Mediterranean, A revision*, Rivista Italiana di Paleontologia e Stratigrafia, Milano, 81, 527-566.
- Cita M.B., Santambrogio S., Melillo B., Rogate F. (1990), *Messinian paleoenvironments: new evidence from the Tyrrhenian sea (ODP Leg 107)*, In: Kastens K.A., Mascle J., et al. (Eds.), Proceedings Ocean Drilling Program. Scientific Results, 107, 211–227. DOI: 10.2973/odp.proc.sr.107.161.1990.
- Cloetingh S., Burov E., Poliakov A. (1999), *Lithosphere folding: Primary response to compression? (from central Asia to Paris basin)*, *Tectonics*, 18, NO. 6, 1064-1083. DOI: 10.1029/1999TC900040.
- Critelli S. (2018), *Provenance of Mesozoic to Cenozoic circum-Mediterranean sandstones in relation to tectonic setting*, Earth-Science Reviews, *185*, 624–648. DOI: 10.1016/j.earscirev.2018.07.001.
- Critelli S., Muto F., Perri F., Tripodi V. (2017), *Interpreting provenance relations from sandstone detrital modes, southern Italy foreland region: Stratigraphic record of the Miocene tectonic evolution*, Marine and Petroleum Geology, 87, 47–59. DOI: 10.1016/j.marpetgeo.2017.01.026.
- Critelli S. (2018), *Provenance of Mesozoic to Cenozoic circum-Mediterranean sandstones in relation to tectonic setting*, Earth-Science Reviews, *185*, 624–648. DOI: 10.1016/j.earscirev.2018.07.001.
- Dannowski A., Kopp H., Klingelhoefer F., Klaeschen D., Gutscher M.-A.A., Krabbenhoeft A., Dellong D., Rovere M., Graindorge D., Papenberg C., Klaucke I., (2019), *Ionian abyssal plain: a window into the tethys oceanic lithosphere*, Solid Earth 10, 447–462. DOI: 10.5194/se-10-447-2019.
- Del Ben A., Barnaba C., Taboga A. (2008), *Strike-slip systems as the main tectonic feauteres in the Plio-Quaternary kinematics of the Calabrian Arc*, Marine Geophysical Research, 29, 1-12. DOI: 10.1007/s11001-007-9041-6.
- Del Ben A. (2009), *Earthquakes and shallow structures in south Adria: evidence of recent inversion tectonics*, Nova Science Publishers, Inc, Chapter 6, 147-163.
- Del Ben A., Geletti R., Mocnik A. (2010), *Relation between recent tectonic and inherited Mesozoic structures of the central-southern Adria plate*, Bollettino di Geofisica Teorica ed Applicata, 51, n. 2-3, 99-115.
- Del Ben A., Mocnik A., Volpi V., Karvelis P. (2015), *Old domains in the South Adria plate and their relationship with the West Hellenic front*, Journal of Geodynamics, 89, 15-28. DOI: 10.1016/j.jog.2015.06.003.
- Dellong D., Kilingelhofer F., Kopp H., Graindorge D., Margheriti L., Moretti M., Murphy S., Gutscher M.-A. (2018), *Crustal Structure of the Ionian Basin and Eastern Sicily Margin: Result From a Wide-Angle Seismic Survey*, Journal of Geophysical Research: Solid Earth, 123. DOI: 10.1002/2017JB015312.
- De Voogd B., Truffert C., Chamot-Rooke N., Huchon P., Lallemant S., Le Pichon X. (1992), *Two-ship seismic soundings in the basins of the Eastern MediterraneanSea (Pasiphae Cruise)*, Geophys. Surv. Int., 109, 536–552. DOI: 10.1111/j.1365-246X.1992.tb00116.x.

- Dewey J.F., Pitman III W.C., Ryan W.B.F., Bonnin J. (1973), *Plate tectonics and the evolution of the Alpine system*, Bulletin of the Geological Society of America 84 (10), 3137–3180. DOI: 10.1130/0016-7606(1973)84%3C3137:PTATEO%3E2.0.CO;2.
- Dewey J.F., Helman M.L., Turco E., Hutton D.H.W., Knott S.D. (1989), *Kinematics of the Western Mediterranean*. In: Coward M.P., Dietrich D., Park R.G. (Eds.), Alpine Tectonics: Geological Society Special Publication, 45, 265–283. DOI: 10.1144/GSL.SP.1989.045.01.15.
- Doglioni C., Mongelli F., Pieri P. (1994), *The Puglia uplift (SE Italy): an Anomaly in the foreland of the Apenninic subduction due to buckling of a thick continental lithosphere*, Tectonics, 13, NO. 5, 1309-1321. DOI: 10.1029/94TC01501.
- Doglioni C., Merlini S., Cantarella G. (1999), *Foredeep geometries at the front of the Apennines in the Ionian Sea (central Mediterranean)*, Earth and Planetary Science Letters, 168, 243-254. DOI: 10.1016/S0012-821X(99)00059-X.
- EMODnet Digital Bathymetry (DTM) (2020). DOI: 10.12770/bb6a87dd-e579-4036-abe1-e649cea9881a.
- Faccenna C., Becker T.W., Lucente P., Jolivet L., Rossetti F. (2001), *History of subduction and back-arc extension in the central Mediterranean*, Geophys. J. Int., 145,809–20. DOI: 10.1046/j.0956-540x.2001.01435.x.
- Faccenna C., Piromallo C., Crespo-Blanc A., Jolivet L. (2004), *Lateral slab deformation and the origin of the western Mediterranean arcs*, Tectonics, 23, TC1012. DOI: 10.1029/2002TC001488.
- Faccenna C., & Becker T.B. (2010), *Shaping mobile belts by small-scale convection*, Nature 465, 602-605. DOI: 10.1038/nature09064.
- Filice F., Seeber L., (2019), *The culmination of an Oblique Time-Transgressive Aarc Continent Collision: the Pollino Massif Between Calabria and the Southern Apennines*, *Ital,* Tectonics, 38, 3261–3280. DOI: 10.1029/2017TC004932.
- Ferranti L., Burrato P., Pepe F., Santoro E., Mazzella M.E., Morelli D., Passaro S., Vannucci G. (2014), An active oblique-contractional belt at the transition between the Southern Apennines and Calabrian Arc: The Amendolara Ridge, Ionian Sea, Italy, Tectonics, 33, 2169-2194. DOI: 10.1002/2014TC003624.
- Finetti I., (1982), *Structure, stratigraphy, and evolution of central Mediterranean*, Boll. Geofis. Teor. App., 24, 247-312.
- Finetti I.R., Papanikolaou D., Del Ben A., Karvelis P., (1991), *Preliminary geotectonic interpretation of the East Mediterranean Chain and the Hellenic Arc*, In: Proceedings of the 5th Congress of the GSG, Thessaloniki, May, 1990, Bull.Geol. Soc. Greece 24/1, pp 509–526.
- Finetti I. R. and Del Ben A. (2005), *Crustal tectono-stratigraphic setting of the Adriatic Sea from new CROP seismic data*, CROP PROJECT*:* Deep seismic exploration of the Central Mediterranean and Italy*,* chapter 23, 519–547.
- Frisch, Meschede and Blakey (2011), *Plate Tectonics*, Springer Heidelberg Dordrecht London New York.
- Frizon de Lamotte D., Saint Bezar B., Bracène R. (2000), *The two main steps of the Atlas building and geodynamics of the Western Mediterranean*, Tectonics 19 (4), 740–761. DOI:
- Frizon de Lamotte D., Raulin C., Mouchot N., Wrobel-Daveau J.-C., Blanpied C., Ringenbach J.-C. (2011), *The southernmost margin of the Tethys realm during the Mesozoic and Cenozoic: initial geometry and timing of the inversion processes*, Tectonics 30, 1–22. DOI: 10.1029/2010TC002691.
- Gallais F., Gutscher M.-A., Klaeschen D., Graindorge D. (2012), *Two-stage growth of the Calabrian accretionary wedge in the Ionian Sea (Central Mediterranean): Constraints from*

depht-migrated multichannel seismic data, Marine Geology 326-328, 28-45. DOI: 10.1016/j.margeo.2012.08.006.

- Gallais F., Graindorge D., Gutscher M.-A., Klaeschen D. (2013), *Propagation of a lithospheric tear fault (STEP) through the western boundary of the Calabrian accretionary wedge offshore eastern Sicily (Southern Italy)*, Tectonophysics, 602, 141-152. DOI: 10.1016/j.tecto.2012.12.026.
- García-Mondéjar J. (1989), *Strike-slip Subsidence of the Basque-Cantabrian Basin of Northern Spain and its Relationship to Aptian-Albian Opening of Bay of Biscay*. In: Tankard AJ, Balkwill HR (eds) Extensional Tectonics and Stratigraphy of the North Atlantic Margins, American Association of Petroleum Geologist, Memoir 46, 395–409.
- Gueguen E., Doglioni C., Fernandez M. (1998), *On the post-25 Ma geodynamic evolution of the western Mediterranean, Tectonophysics*, 298, 259-269. DOI: 10.1016/S0040-1951(98)00189-9.
- Gutscher M.-A., Domininguez S., Mercier de Lepinay B., Pinheiro L., Gallais F., Babonneau N. et al. (2015), *Tectonic expression of an active slab tear from high-resolution seismic and bathymetric data offshore Sicily (Ionian Sea)*, Tectonics, 34. DOI: 10.1002/2015TC003898.
- Handy M.R., Schmid M., S, Bousquet R., Kissling E., Bernoulli, D., (2010), *Reconciling plate-tectonic reconstructions of Alpine Tethys with the geological–geophysical record of spreading and subduction in the Alps*, Earth Sci. Rev. 102, 121–158. DOI: 10.1016/j.earscirev.2010.06.002.
- Handy M. R., Giese J., Schmid S. M., Pleuger J., Spakman W., Onuzi K., & Ustaszewski K. (2019), *Coupled crust-mantle response to slab tearing, bending, and rollback along the Dinaride-Hellenide orogen*, Tectonics, 38, 2803–2828. DOI:10.1029/ 2019TC005524.
- Hieke W., Hirschleber H.B., Dehghani A. (2003), The Ionian Abyssal Plain (central Mediterranean Sea): Morphology, subbottom structures and geodynamic history – An inventory, Marine Geophysical Research, 24(3):279-310. DOI: 10.1007/s11001-004-2173-z.
- Jackson J., McKenzie D.P. (1988), *The relationship between plate motions and seismic moments tensors, and the rates of active deformation in the Mediterranean and Middle East*, Geophys. J. Int., 93, 45–73. DOI: 10.1111/j.1365-246X.1988.tb01387.x.
- ISIDe Working Group (2007), *Italian Seismological Instrumental and Parametric Databas*e (ISIDe). DOI: doi.org/10.13127/ISIDE
- Jolivet L., Faccenna C. (2000), *Mediterranean extension and the Africa-Eurasia collision*, Tectonics, 19,1095–106. DOI: 10.1029/2000TC900018.
- Jolivet L., Menant A., Roche V., Le Pourhiet L., Maillard A., Augier R., Do Couto D., Gorini C., Thinon I., Canva A. (2021), *Transfer zones in Mediterranean back-arc regions and tear faults*, Bulletin de la Société Géologique de France, 192 (1), 11. DOI: 10.1051/bsgf/2021006.
- Kamberis E., Ioakim Ch, St T-M, Tsapralis V. (1992), *Geodynamic and palaeogeographic evolution of western Peloponnesus (Greece) during the Neogene*, Paleontologia I Evolucio 24–25, 363–376.
- Kamberis E., Marnelis F., Loucoyannakis M., Maltezou F., Hirn A., Streamers Group (1996), *Structure and Deformation of the External Hellenides Based on Seismic Data from Offshore Western Greece*, EAGE Special Publication, 5,207–214.
- Kamberis E., Ioakim Ch., St T-M, Marnelis F., Sotiropoulos S. (1998), *Geologic and Paleogeographic evolution of Western Greece during the Neogene—Quaternary period in the geodynamic setting of the Hellenic Arc*, Roman J Stratigraphy, 78:63–73.
- Kamberis E., Kokinou E., Florika Koci f., Katerina Lioni k., Alves TM., Velaj T. (2021), *Triassic evaporites and the structural architecture of the External Hellenides and Albanides (SE Europe): controls on the petroleum and geoenergy systems of Greece and Albania*, International Journal of Earth ScienceS. DOI: 10.1007/s00531-021-02151-4.
- Kilias A., Tranos M., Mountrakis D., Shallo M., Marto A., Turku I. (2001), *Geometry and kinematics of deformation in the Albanian orogenic belt during the Tertiary*, J. Geodyn 31(2), 169–187.

- Koyi H. (1998), *The shaping of salt diapirs*, Journal of Structural Geology, 20, 321-338. DOI: 10.1016/S0191-8141(97)00092-8.
- Kopf A., Mascle J., Klaeschen D. (2003), *The Mediterranean Ridge: A mass balance across the fastest growing accretionary complex on Earth,* Journal of Geophysical Research, 108, 2372. DOI: 10.1029/2001JB000473.
- Krijgsman W., Hilgen F.J., Raffi I., Sierro F.J., Wilson D.S. (1999), *Chronology, causes and progression of the Mediterranean salinity crisis*, Nature, 400, 652–655.
- Lay T. (2015), *The surge of great earthquakes from 2004 to 2014*, Earth and Planetary Science Letters, 409, 133-146. DOI: 10.1016/j.epsl.2014.10.047.
- Le Breton E., Handy M.R., Molli G. and Ustaszewski K. (2017), *Post-20 Ma motion of the Adriatic plate – new constrains from surrounding orogens and implications for crust-mantle decoupling*, Tectonics, 36. DOI: 10.1002/2016TC004443.
- Le Pichon X., Angelier J., (1979), *The Hellenic arc and trench system: a key to the neotectonic evolution of the Eastern Mediterranean area*, Tectonophysics, 60,1–42. DOI: 10.1016/0040-1951(79)90131-8.
- Le Pichon X., Lallemant SJ., Chamot-Rooke N., Lemeur D., Pascal G. (2002), *The Mediterranean Ridge backstop and the Hellenic nappes*, Mar. Geol., 186, 111-125.
- Locati M., Camassi R. D., Rovida A. N., Ercolani E., Bernardini F. M. A., Castelli V., et al. (2016), *DBMI15, the 2015 version of the Italian Macroseismic Database*, edited, Istituto Nazionale di Geofisica e Vulcanologia. DOI: https://doi.org/10.6092/INGV.IT-DBMI15
- Lòpez-Gòmez J., Alfondo-Azcàrate J., Arche A., Arribas J., Fernàndez Barrenechea J., Borruel-Abadìa V., Bourquin S., Cadenas P., Cuevas J., De la Horra R., Bienvido Dìez J., Escudero-Mozo M. J., Fernàndez-Viejo G., Gàlan-Abellàn B., Galè C., Gaspar-Escribano J., Gisbert Aguilar J., Gòmez-Gras D., Goy A., Gretter N., Carballo M. P., Lago M., Lloret J., Luque J., Màrquez L., Màrquez-Aliaga A., Martin-Algarra A., Martin-Chivelet J., Martìn-Gonzàles F., Marzo M., Mercedes-Martin R., Ortì F., Pèrez-Lòpez A, pèrez-Valera F., Pèrez-Valera J. A., Plasencia P., Ramos E., Rodrìguez-Mèndez L., Ronchi A., Salas R., Sànchez-fernàndez d., sànchez-Moya Y., Sope˜na A., Suàrez-Rodrìguez A'., Tubìa J. M., Ubide T., Garcès B. V., Vargas H., Viseras C. (2019), *Permian-Triassic Rifting Stage*, The Geology of Iberia: A Geodynamic Approach, Regional Geology Reviews. DOI: 10.1007/978-3-030-11295-03.
- Maesano F.E., Tiberti M.M., Basili R. (2017), *The Calabrian Arc: three dimensional modelling of the subduction interface*, Scientific Reports. DOI: 10.1038/s41598-017-09074-8.
- Maesano F.E., Volpi V., Civile D., Basili R., Conti A., Tiberti M.M., Accettella D., Conte R., Zgur F., Rossi G (2020)., *Active Extension in a Foreland Trapped Between Two Contractional Chains: The South Apulia Fault System (SAFS)*, Tectonics, 39, 2020TC006116. DOI: 10.1029/2020TC006116.
- Malinverno A. and Ryan W.B.F. (1986), *Extension in the Tyrrhenian Sea and shortening in the Apennines as results of arc migration driven by sinking of the lithosphere*, Tectonics, 5, 227-245. DOI: 10.1029/TC005i002p00227.
- Manzi V., Argnani A., Corcagnani A., Lugli S., Roveri M. (2020), *The Messinian salinity crisis in the Adriatic foredeep: Evolution of the largest evaporitic marginal basin in the Mediterranean*, Marine and Petyroleum Geology, 115, 104288. DOI: 10.1016/j.marpetgeo.2020.104288.
- Marnelis F., Roussos N., Rigakis N., Karakitsios V. (2007), *Structural geology of the western Greece fold-and-thrust belt*, AAPG and AAPG European Region Energy Conference and Exhibition 2007, Athens, Greece, November 14–17, Guide to Fieldtrip, 1, 1–29.
- Mattavelli L., Novelli L., Anelli L. (1991), *Occurrence of hydrocarbons in the Adriatic basin*. In: Spencer (Ed.), Generation, Accumulation, and production of Europe's Hydrocarbons. Sp. Publ. of the European Association of Petroleum Geoscientists, 369–380.

- Mavromatidis A., Kelessidis V.C., Monopolis D.G. (2004), *A review of recent hydrocarbon exploration in Greece and its potential*, 1st International Conference on Advances in Mineral Resource Management and Environmental Geotechnology, Chania, Greece, June 7–9, 1–8.
- Merlini S., Cantarella G., Doglioni C. (2000), *On the seismic profile Crop M5 in the Ionian Sea*, Boll. Soc. Geol. It., 119, 227-236, 7 ff.
- Mila A., Torrente M.M., Iannace P. (2017), *Pliocene-Quaternary orogenic systemb in central Mediterranean,: the apulia-southern Apennines-Tyrrhenian Sea example*, Tectonics, 1-19. DOI: 10.1002/2017tc004571.
- Minelli L. and Faccenna C. (2010), *Evolution of the Calabrian accretionary wedge (central Mediterranean)*, Tectonics, 29, TC 4004. DOI: 10.1029/2009TC002562.
- McKenzie D. (1978), *Some remarks on the development of sedimentary basins.Earth Planet*, Sci. Lett., 40, 25–32. DOI: 10.1016/0012-821X(78)90071-7.
- Moretti A. and Royden L. (1988), *Deflection, gravity anomalies and tectonics of doubly subducted continental lithosphere: adriatic and ionian seas*, Tectonics, 7, 875-893. DOI: 10.1029/TC007i004p00875.
- Mostardini F., Merlini, S. (1986), *Appennino centro-meridionale Sezioni geologiche e proposta di modello strutturale*, Mem. Soc. Geol. It, 35, 59.
- Nicolai C. and Gambini R. (2007), *Structural architecture of the Adria platform-and-basin system*, Boll. Soc. Geol. It. (Ital.J.Geosci.), Spec. Issue, 7, 21-37.
- Patacca E., Sartori R. and Scandone P. (1990), *Tyrrhenian basin and Apenninic arcs: Kinematic relation since Late Tortonian times*, Mem. Soc. Geol. Ital., 45, 425-451.
- Patacca E.& Scandone P. (2007), *Geology of the Southern Apennines*, Boll. Soc. Geol.It. (*Ital.J.Geosci.*), Spec. Issue No. 7, pp. 75-119.
- Patacca E., Scandone, P., Di Luzio E., Cavinato G.P., Parotto M. (2008), *Structural architecture of the central Apennines: Interpretation of the CROP 11 seismic profile from the Adriatic coast to the orographic divide*, Tectonics, 27, TC3006. DOI: 10.1029/2005TC001917.
- Pellen R., Aslanian D., Rabineau M., Suc J.-P., Cavazza W., Popescu S.-M., Rubino J.-L. (2022), *Structural and sedimentary origin of the Gargano - Pelagosa gateway and impact on sedimentary evolution during the Messinian Salinity Crisis*, Earth-Science Reviews. Doi: https://doi.org/10.1016/j.earscirev.2022.104114.
- Pieri P., Vitale G., Beneduce P., Doglioni C., Gallicchio S., Giano S.I., Loizzo R., Moretti M., Prosser G., Sabato L., Schiattarella M., Tramutoli M., Tropeano, M. (1997), *Quaternary tectonics in the Bradanic-lonian area / Tettonica quaternaria nell'area bradanico-ionica*, Italian Journal of Quaternary Sciences 10(2), 535-542.
- Polonia A., Torelli L., Mussoni P., Gasperini L., Artoni A., Klaeschen D., (2011), *The Calabrian Arc subduction complex in the Ionian Sea: Regional architecture, active deformation, and seismic hazard*, Tectonics, 30, TC5018. DOI: 10.1029/2010TC002821.
- Polonia A., Torelli L., Gasperini L., Mussoni P. (2012), *Active faults and historical earthquakes in the Messinian strait area (Ionian Sea)*, Nat. Hazards Earth Syst. Sci., 12, 2311-2328. DOI: 10.5194/nhess-12-2311-2012.
- Polonia A., Torelli L., Artoni A., Carlini M., Faccenna C., Ferranti C., Gasperini L., Govers R., Klaeschen D., Monaco C., Neri G., Nijholt N., Orecchio B., Wortel R. (2016), *The Ionian and Alfeo-Etna fault zones: New segments of an evolving plate boundary in the central Mediterranean sea?*, Tectonophysics, 675, 69-90. DOI: 10.1016/j.tecto.2016.03.016.
- Ricchetti G., Ciaranfi N., Luperto Sinni E., Mongelli F., Pieri P., (1988), *Geodinamica ed evoluzione sedimentaria e tettonica dell'Avampaese Apulo*, Mem. Soc. Geol.It., 41, 57–82.
- Rossi S., Borsetti A.M. (1974), *Dati preliminari di stratigrafia e di sismica del Mare Ionio settentrionale*, Mem. Soc. Geol. It, 13/2, 251e259.
- Rossi S. and Sartori. R. (1981), *A seismic reflection study of the external Calabrian Arc in the Norther Ionian Sea (Eastern Mediterranean)*, Marine Geophysical Researches, 4, 403-426. DOI: 10.1007/BF00286036.

- Rouchy J.-M., Orszag- Sperber F., Blanc-Valleron M.-M., Pierre C., Rivière M., Combourieu-Nebout N. & Panayides I. (2001), *Paleoenvironmental changes at the Messinian-Plioceneboundary in the eastern Mediterranean: southern Cyprus basins*, Sedimentary Geology, 145, 93-117. DOI: 10.1016/S0037-0738(01)00126-9.
- Rovida A., Locati M., Camassi R., Lolli B., & Gasperini P. (Eds.) (2016), *Catalogo Parametrico dei Terremoti Italiani (CPTI15)*, Istituto Nazionale di Geofisica e Vulcanologia (INGV). DOI: https://doi.org/10.6092/INGV.IT-CPTI15.
- Royden L. and Faccenna C. (2018), *Subduction Orogeny and the Late Cenozoic Evolution of the Mediterranean Arcs, Annual Review of Earth and Planetary Sciences*, 46:216-89. DOI: 10.1146/annurev-earth-060115-012419.
- Royden L. H., and Papanikolaou D. J. (2011), *Slab segmentation and late Cenozoic disruption of the Hellenic arc*, Geochem. Geophys. Geosyst., 12, Q03010. DOI: 10.1029/2010GC003280.
- Roveri M., Flecker R., Krijgsman W., Lofi J., Lugli S., Manzi V., J. Sierro F., Bertini A., Camerlenghi A., De Lange G., Govers R., J. Hilgen F., Hübscher C., Th.Meijer P., Stoica M. (2014), *The Messinian Salinity Crisis: Past and future of a great challenge for marine sciences*, Marine Geology, 352, 25–58. DOI: 10.1016/j.margeo.2014.02.002.
- Roussos N, Marnelis F (1995), *Greece licensing round to focus on Western sedimentary basins*, Oil Gas J 93(10):58–62.
- Sabbatino M, Vitale S, Tavani S., Consorti L., Corradetti A., Cipriani A., Arienzo I., Parente M., (2020), *Constraining the onset of flexural subsidence and peripheral bulge extension in the Miocene foreland of the southern Apennines (Italy) by Sr-isotope stratigraphy*, Sedimentary Geology, Volume 401, 105634. DOI: 10.1016/j.sedgeo.2020.105634.
- Sartori R. (1990), *The main results of ODP leg 107 in the frame of neogene to recent geology of perityrrhenian areas*, in Proc. Ocean Drilling Program, Sci. Results, 107, 715-730. DOI: 10.2973/odp.proc.sr.107.183.1990
- Sartori R. (2003), *The Tyrrhenian back-arc basin and subduction of the Ionian lithosphere*, Episodes, 26, 217-221.
- Schmid S. M., Bernoulli D., Fügenschuh B., Matenco L., Schuster R., Schefer S., et al. (2008), *The Alpine-Carpathian-Dinaridic orogenic system: Correlation and evolution of tectonic units*, Swiss Journal of Geosciences, 101(1), 139–183. DOI: 10.1007/s00015-008-1247-3
- Sciuto F., Baldanza A. (2020), *Full restoration of marine conditions after the late Messinian Mediterranean Lago-Mare phase in Licodia Eubea and Villafranca Tirrena areas (east Sicily),* Carnets Geol. 20 (6). DOI: 10.4267/2042/70760.
- Senatore MR., Normark WR., Pescatore T., Rossi S. (1988), *Structural framework of the Gulf of Taranto (Ionian Sea)*, Boll. Soc. Geol. It., 41, 533-539.
- Speranza F., Minelli L., Pignatelli A., Chiappini M. (2012), *The Ionian Sea: the oldest in situ ocean fragment of the world?* J. Geophys. Res. 117. DOI: 10.1029/2012JB009475.
- Stampfli G., Borel G. (2002), *A plate tectonic model for the Paleozoic and Mesozoic constrained by dynamic plate boundaries and restored synthetic oceanic isochrons*, Earth Planet Sci. Lett. 196, 17–33. DOI: 10.1016/S0012-821X (01)00588- X.
- Stampfl G.M. (2005), *Plate Tectonics of the Apulia-Adria Microcontinents*, CROP PROJECT*:* Deep seismic exploration of the Central Mediterranean and Italy, chapter 33, 747-765.
- Stern R.J., (2002), *Subduction Zones*, Reviews of Geophysics, 40, 4.
- Sukumono S. and Ambarsari D.S. (2019), *Practical Seismic Interpretation for Petroleum Exploration*, ITB Press.
- Tortorici L. (1982), *Lineamenti geologico strutturali dell'Arco Calabro-Peloritano, Società Italiana di Mineralogia e Petrologia*, 38 (3), 927-940.
- Tropeano M., Sabato L., Pieri P. (2002), *Filling and cannibalization of a foredeep: The Bradanic Trough, southern Italy*, Geol. Soc. Spec. Publ., 191, 55-79. DOI: 10.1144/GSL.SP.2002.191.01.05.

- Tropeano M., Spalluto L., Meloni D., Moretti M., Sabato L. (2022), *Isolated base-of-slope aprons': An oxymoron for shallow-marine fan-shaped, temperate-water, carbonate bodies along the south-east Salento escarpment (Pleistocene, Apulia, southern Italy)*, Sedimentology, 69, 345–371. DOI: 10.1111/sed.12941.

- Tugend J., Chamot-Rooke N., Arsenikos S., Blanpied C, Frizon de Lamotte D., (2019), Geology of the Ionian Basin and margins: a key to the East Mediterranean geodynamics, Tectonics, 38 (8), 2668-2702. DOI: 10.1029/2018TC005472.
- Vai G.B. (1994), *Crustal evolution and basement elements in the Italian Area: palaeogeography and characterization*, Boll. Geof. Teor. Appl., 36 (141–144),411–434.
- Vail P.R. (1987), Seismic stratigraphy interpretation using sequence stratigraphy, AAPG Stud. Geol. 27, 1 Atlas Seism. Stratigr. 1, 1-10.
- Van Dijk J.P., Scheepers P.J.J. (1995), *Neotectonic rotations in the Calabrian Arc;implications for a Pliocene-recent geodynamic scenario for the Central Mediterranean*, Earth. Sci. Rev., 39, 207–246. DOI: 10.1016/0012-8252(95)00009-7.
- Van Hinsbergen D.J.J., Torsvik T.H., Schmid S.M., Matenco L.C., Maffione M., Vissers R.L.M., Gürer D., Spakman W. (2020), *Orogenic architecture of the Mediterranean region and kinematic reconstruction of its tectonic evolution since the Triassic*, Gondwana Res., 81, 79–229. DOI: 10.1016/j.gr.2019.07.009.
- Vitale S., Ciarcia S. (2013), *Tectono-stratigraphic and kinematic evolution of the southern Apennines/Calabria–Peloritani Terrane system (Italy)*, Tectonophysics, 583, 164–182. DOI: 10.1016/j.tecto.2012.11.004.
- Volpi V., Accettella D., Cuppari A. (2011). *Morphological features of the Apennines foreland/accretionary-wedge boundary in the Ionian Sea*, Mar. Geophys. Res., 32, 481-492. DOI: 10.1007/s11001-011-9140-2.
- Volpi V., Del Ben A., Civile D., Zgur F. (2017), *Neogene tectono-sedimentary interaction between the Calabrian Accretionary Wedge and the Apulian Foreland in the northern Ionian Sea,* Marine and Petroleum Geology, 83, 246-263. DOI: 10.1016/j.marpetgeo.2017.03.013.
- Wang K. and Trènu A. (2016), *Some outstanding issues in the study of great megathrust earthquakes-The Cascadia example*, Journal of Geodynamics, 98, 1-18. DOI: 10.1016/j.jog.2016.03.010.
- Zecchin M., Praeg D., Ceramicola S., Muto F. (2015), *Onshore to offshore correlation of regional unconformities in the Plio-Pleistocene sediemntary succession of the Calabrian Arc (central Mediterranean)*, Earth-Science Reviews, 142, 60-78. DOI: 10.1016/j.earscirev.2015.01.006.
- Zecchin M., Civile D., Caffaua M., Critelli S., Muto F., Manganoa G., Ceramicola S. (2020), *Sedimentary evolution of the Neogene-Quaternary Crotone Basin (southern Italy) and relationships with large-scale tectonics: A sequence stratigraphic approach*, Marine and Petroleum Geology, 117. DOI: 10.1016/j.marpetgeo.2020.104381.
- Zelilidis A., Piper DJW., Vakalas I., Avramidis P., Getsos K. (2003), *Oil and gas plays in Albania: do equivalent plays exist in Greece?*, Journal of Petroleum Geology, 26(1), 29–48.
- Zelilidis A., Maravelis A.G., Tserolas P., Konstantopoulos P.A. (2015), *An overview of the petroleum systems in the Ionian Zone, onshore NW Greece and Albania*, Journal of Petroleum Geology, 38(3), 331-348. DOI: 10.1111/jpg.12614.

FIGURES CAPTIONS

Fig. 1: location of the study area in the Central Mediterranean Sea region and tectonic evolution of the western-central Mediterranean from 30 Ma to Present with major paleogeographic features involved in this kinematic setting (a-e). During Late Oligocene-Middle Miocene time the CA was located adjacent to Sardinia block. Since Late Miocene, the CA has migrated toward SE due to subduction roll-back of the Ionian oceanic lithosphere, coeval opening of the Tyrrhenian basin and collision with Apulia and Africa to produce the CA wedge, the Apenninic and Maghrebian orogenic belts (after Capozzi et al., 2012).

Fig. 2: main geological domains and structural setting of the Northern Ionian Sea (after Basso et al., 2021). The study area is represented by the dashed blue line. Red arrow is the slip vector between Africa and Europe in the Europe-fix reference frame and the yellow arrows are the GPS vectors in the Africa/Nubia-fix reference frame (D'Agostino et al., 2008).

Fig. 3: (a) schematic stratigraphic columns of the CA wedge (1) and of the Apulian foreland (2), reconstructed on the base of the available literature (after Volpi et al., 2017); (b) stratigraphic columns for the the Albanian-Hellenic zone (1) and Plio-Quaternary synthetic lithological column of Western Greece (2)(after Zelilidis et al., 2003, 2015; Kamberis et al, 2021); (c) schematic representation of the three

main unconformities (MPCU, EPSU, MPSU) and related Plio-Pleistocene tectono-sedimentary cycles (P1-P4) in the CA and Bradano Basin (1) and the Neogene stratigraphic units recognized in this work and related to those identified by Basso et al. (2021) (2) (after Zecchin et al., 2015 in Basso et al., 2021).

Fig. 4: bathymetric map of the study area provided by EMODet Bathymetry Consortium (DTM 2018) (https://www.seadatanet.org/) dataset available for the study area and location of the seismic lines selected and interpreted in this work, labelled Line 1 to Line 4 (red lines). The related domains intercepted by seismic lines are indicated.

Fig. 5: different seismic sequences and topping horizons identified on the Apulian foreland; (a) the Upper Plio-Holocene/Lower Pliocene boudary is represented by the MPCU; see the semi-transparent feature of the Lower Pliocene (detail of Line 2); (b) Cretaceous-Jurassic boundary, well define by an uncoformity with onlap geometries ; the basin to platform facies transition is defined by the blue dashed line (detail of Line 1); (c) the chaotic-blind seismic facies in the Jurassic sequence, where the seismic signal is almost wipe-out (detail of Line 2); (d) the Jurassic/Upper Triassic boundary is defined by an high-amplitude reflector; the top of the Lower Triassic-Upper Permian is highlighted, defining the possible base of the sedimentary cover above the crystalline basement (detail of Line 1).

Fig. 6: (a) Seismic Line 1; see the location in Fig.4; (b) Upper Plio-Holocene-Lower Pliocene onlap in the CA wedge; here, the MPCU, the EPSU and the MPSU are clear

an traced; (c) extensional tectonics in the foreland associated to escarpments and syn-tectonic wedeges; (d) positive bulges (B1,B2,B3) associated to recent tectonic positive inversion processes affecting the foreland seabed; (e) collision between the CA wedge front and the Apulian foreland in the Northern Ionian Sea and the adjacent Bradano foredeep basin; see the subducted inverted faults deforming the sole thust (SIF1 to SIF 5); (f) the Upper Plio-Holocene package sediments, onlap the apulian monocline in the Bradano foredeep basin; Here, the MPCU, EPSU and MPSU are clear and traced, as well as the Mesozoic unconformity.

Fig. 7: (a) Seismic Line 2; see the location in Fig. 4; (b) active extensional tectonics in the SSW sector of this line, associated with seabed escarpments; the blue dashed line represents sectors where the continuity of the carbonate platform reflectors appears interrupted; (c) a prominent horst structure (HS) surronded by the Northern Basin (NB) and the Southern Basin (SB) shows a folded geometry of the pre-Pliocene seismic sequence suggests the presence of a previous positive flower structure (PF1); (d) the lowermost portion of the Upper Plio-Holocene sequence (Post MPCU) corresponds to the strike slip basin related to the PF1 strike-slip structure (note the onlap geometries on both sides of the confined basin and the SSW-ward onlap against folded reflections related to dashed reverse faults); on the other hand, the Upper Plio-Holocene uppermost part (Post MPSU) corresponds to the syn-tectonic wider wedge linked to a more recent extensional tectonics (NNE dipping faults); (e) both the top of the Lower Pliocene and the pre-Pliocene seismic sequences appear folded and associated to antiformal structures (A1-A2), either sealed (A2) or cut (A1) by extensional faults.

Fig. 8: Seismic Line 3; here, transpressive tectonics is evidenced by active positive flower structures associated to seabed deformation (PF4 to PF9) and two positive flower structures deforming the lower Pliocene but sealed by the Upper Plio-Holocene sediments (PF2-PF3); see the location in Fig. 4.

Fig. 9 (a): Seismic Line 4; see the location in Fig.4; (b) nearby the Hellenic foredeep basin, transpressive/compressive tectonics has been identified, evidenced by two positive flower structures (PF2 and PF3), interpreted as inverted older (Mesozoic) extensional faults; in the uppermost part of PF2 and PF3, eight shallower faults associated to reverse offset disrupt the Lower Pliocene seismic sequence; note the Hellenic Upper Pliocene-Holocene sediments-Apulian monocline onlap; here, the MPCU, the EPSU and the MPSU are clearly imaged.

Fig. 10: bathymetric map provided by EMODnet Bathymetry Consortium (DTM 2018) (https://www.seadatanet.org/) showing the main bathymetric features and the recent/active (morpho) structure of the study area; below, the bathymetric profiles obtain using the Global Mapper v. 21 software (http://www.bluemarblegeo.com/). the Profile 1 intercepts the Apulian foreland and both the CA wedge and Hellenic fold/thrust belt; the black arrow indicates the AP bulge generated by the bending; the Profile 2 shows the wedge-top basin (WB) in the upper part of the CA wedge, also mapped in the bathymetric map above. Profile 3 shows the bulges (B1, B2, B3) associated to inverted faults nearby the Bradano foredeep basin, illustrated in Fig. 6c. Profile 4 illustrates the horst structures (HS) as well as the the surrounding basin: the Southern Basin (SB) and Northern Basin (NB) both mapped in this bathymetric map and seismic reflection

profile (Figs 6c and 7c). Profile 5 shows the seabed bulge associated to the positive flower PF4 to PF7 shown in Line 3 (Fig. 8).

Fig. 11: structural maps of the study area obtained by the integration of seismic profiles and bathymetric data provided by EMODnet Bathymetry Consortium (2020) (https://www.seadatanet.org/).

Fig. 12: structural maps obtained by the integration of seismic profiles, bathymetric data provided by EMODnet Bathymetry Consortium (2020) (https://www.seadatanet.org/) and timing of different tectonic structures defined in Figs. 6-7-8-9. The three maps represent the tectonic setting of the study area at different time intervals: (a) Jurassic-Lower Cretaceous / Cretaceous-Upper Miocene, (b) Messinian/Lower Pliocene (pre-MPCU), (c) post-MPCU/pre-MPSU.

Fig. 13: sketchs of the main tectono-stratigraphic evolution of the Apulian foreland investigated in this paper (not in scale); (a) Jurassic / Lower Cretaceous; (a1) Cretaceous / Upper Miocene; (b) Messinian / Lower Pliocene (pre-MPCU); (c) post-MPCU / pre-MPSU; (d) post-MPSU / Holocene.

Fig. 14: (a) curvature of the Apulian foreland along three transects. Note that the area affected by extensional tectonics coincides with the sector of maximum curvature (section B), which correspond to the eastern sector study area (highlighted in orange in the map above) (modified after Argnani et al., 2001); (b) the flexural bending process: the Apulian foreland is deflected in response to the

load applied by the CA wedge and Hellenides and this induces an extensional regime; (c) the lithospheric buckling process: the horizontal stress transmitted by the CA wedge may have contributed to the folding and therefore re-activation of previous extensional fault as reverse.

Fig. 15: the tangential Middle-Upper Pleistocene force components (f_T) due to the advancement of the two opposite wedges favoured a strike slip regime in the central sector of the Apulian foreland, to which the normal compression components (f_N) are added, implying a transpressive regime. Stress orientation according to Mila et al. (2017) and Del Ben et al. (2008).

TABLE

Tab. 1: Characteristics of the selected seismic reflection profiles. The acquisition power is expressed in cubic inches (c.i.) of the Lines 1, 2 and in bar for the Lines 3 and 4 (CROP survey).

ID	Lenght (Km)	Source type	Source power (c.i.)	Source depth (m)	Streamer depth (m)	Streamer lenght (m)	Shotpoint interval (m)	Group interval (m)
Line 1	137,62	Airgun Array	3410	6	8	6000	25	12,5
Line 2	121,96	Airgun Array	3410	6	8	6000	25	12,5
Line 3	133,31	High Pressure Airgun	140 bar	6	12	4500	62,5	25
Line 4	111,52	High Pressure Airgun	140 bar	6	12	4500	62,5	23

Tab. 1: Characteristics of the selected seismic reflection profiles. The acquisition power is expressed in cubic inches (c.i.) of the Lines 1, 2 and in bar for the Lines 3 and 4 (CROP survey).

HIGHLIGHTS

- The response of a subducting plate trapped between two converging orogenic wedge is investigated.
- The interference of Calabrian Arc (CA) and Hellenic chain plays an important role in defining the tectono-stratigraphic evolution of the Apulian Swell (AP) in Central Mediterranean Sea.
- The advancement of the CA wedge and the Hellenides transmitted compressive stress to the foreland, leading to a tectonic inversion of previous Mesozoic faults.
- The CA wedge changes direction of movement in Middle Pleistocene and the consequent oblique convergence drove transpressional tectonics inside the Apulian Swell.
- Compressive deformation at the AP-CA wedge contact zone suggests that the west-dipping AP is already part of the orogenic wedge.
- Compressive tectonics is active also in the central sector of the AP implying that collisional tectonics can be propagated over long distances from plate boundaries.

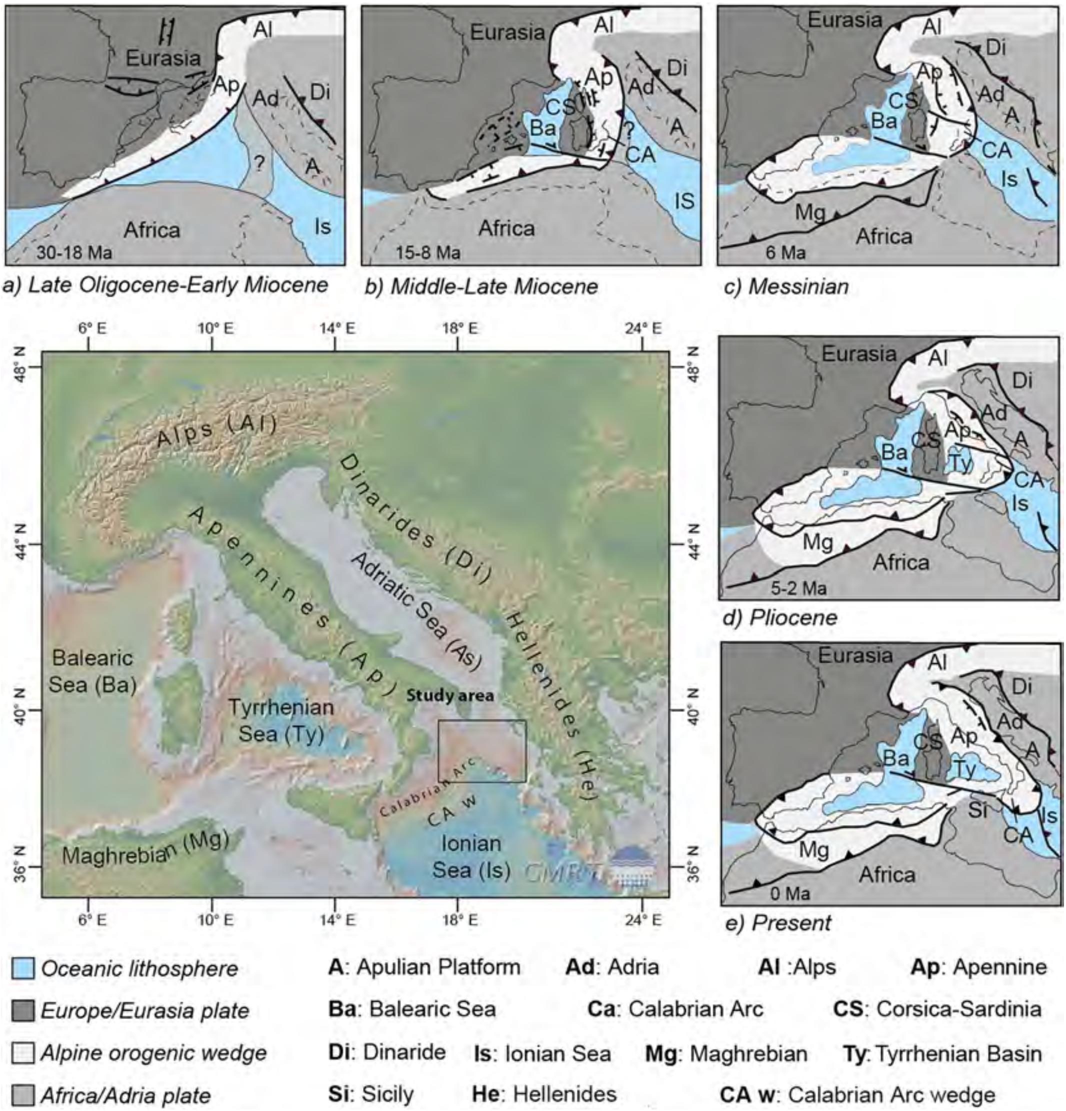

Eurasia
Al
Ap
Ad
Di
?
A
Africa
Is
30-18 Ma
a) Late Oligocene-Early Miocene
Eurasia
Al
Ap
Ad
Di
CS
It
Ba
?
A
CA
IS
Africa
15-8 Ma
b) Middle-Late Miocene
Eurasia
Al
Di
Ap
CS
Ad
Ba
A
CA
Is
Mg
Africa
6 Ma
c) Messinian
6° E
10° E
14° E
18° E
24° E
48° N
44° N
40° N
36° N
Alps (Al)
Dinarides (Di)
Apennines (Ap)
Adriatic Sea (As)
Hellenides (He)
Balearic Sea (Ba)
Tyrrhenian Sea (Ty)
Study area
Calabrian Arc
CA w
Maghrebian (Mg)
Ionian Sea (Is)
GMRT
Eurasia
Al
Di
Ad
Ap
A
Ba
CS
Ty
CA
Is
Mg
Africa
5-2 Ma
d) Pliocene
Eurasia
Al
Di
Ad
Ap
A
CS
Ba
Ty
Si
Is
CA
Mg
Africa
0 Ma
e) Present
Oceanic lithosphere
Europe/Eurasia plate
Alpine orogenic wedge
Africa/Adria plate
A: Apulian Platform
Ad: Adria
Al :Alps
Ap: Apennine
Ba: Balearic Sea
Ca: Calabrian Arc
CS: Corsica-Sardinia
Di: Dinaride
Is: Ionian Sea
Mg: Maghrebian
Ty: Tyrrhenian Basin
Si: Sicily
He: Hellenides
CA w: Calabrian Arc wedge

Figure 1

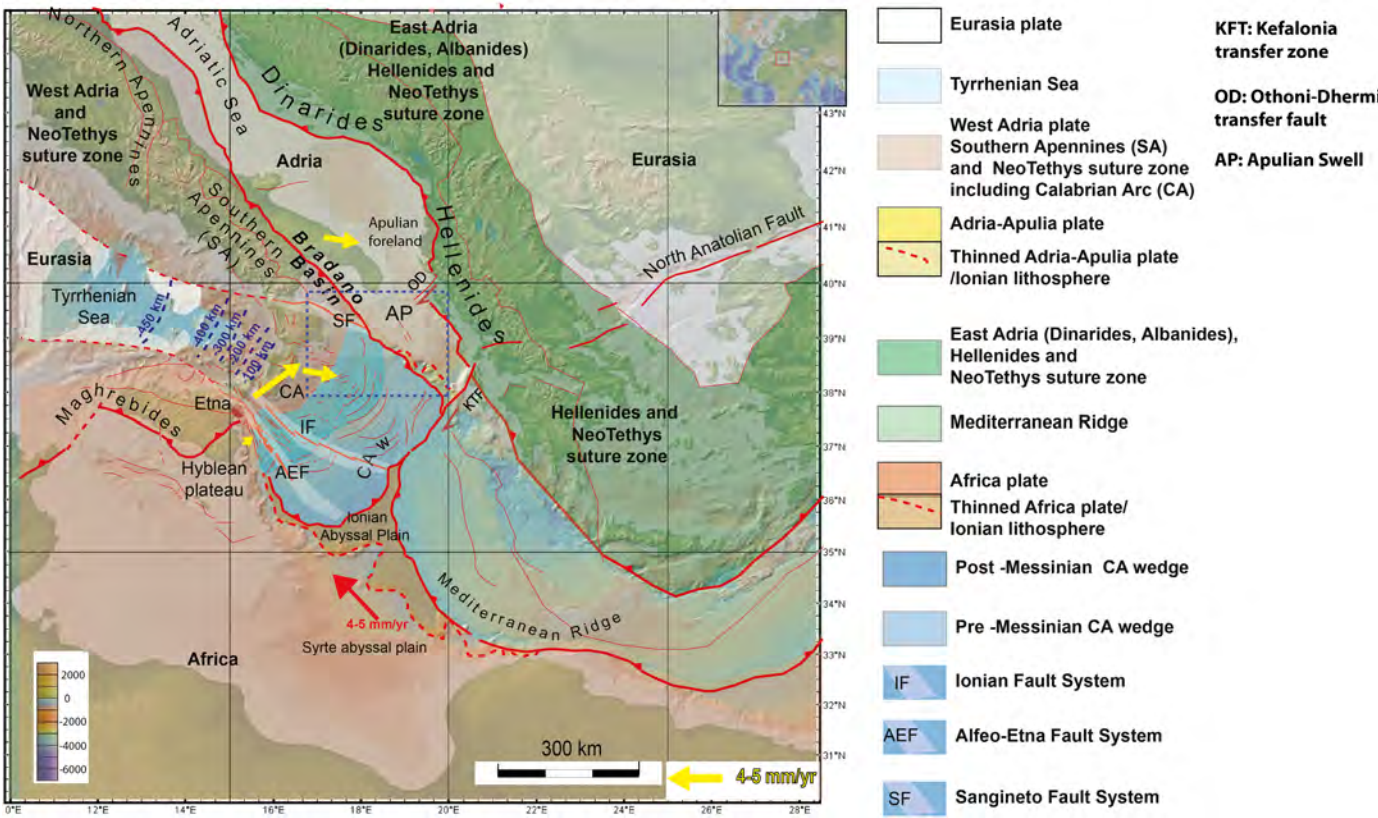
Northern Apennines
Adriatic Sea
Dinarides
East Adria (Dinarides, Albanides) Hellenides and NeoTethys suture zone
West Adria and NeoTethys suture zone
Adria
Eurasia
Apulian foreland
Southern Apennines (SA)
Bradano Basin
Hellenides
North Anatolian Fault
Eurasia
Tyrrhenian Sea
450 km
400 km
300 km
200 km
100 km
OD
SF
AP
CA
Etna
Maghrebides
IF
KTF
CAw
AEF
Hyblean plateau
Hellenides and NeoTethys suture zone
Ionian Abyssal Plain
Mediterranean Ridge
4-5 mm/yr
Syrte abyssal plain
Africa
2000
0
-2000
-4000
-6000
300 km
4-5 mm/yr
Eurasia plate
Tyrrhenian Sea
West Adria plate Southern Apennines (SA) and NeoTethys suture zone including Calabrian Arc (CA)
Adria-Apulia plate
Thinned Adria-Apulia plate /Ionian lithosphere
East Adria (Dinarides, Albanides), Hellenides and NeoTethys suture zone
Mediterranean Ridge
Africa plate
Thinned Africa plate/ Ionian lithosphere
Post -Messinian CA wedge
Pre -Messinian CA wedge
IF Ionian Fault System
AEF Alfeo-Etna Fault System
SF Sangineto Fault System
KFT: Kefalonia transfer zone
OD: Othoni-Dhermi transfer fault
AP: Apulian Swell

Figure 2

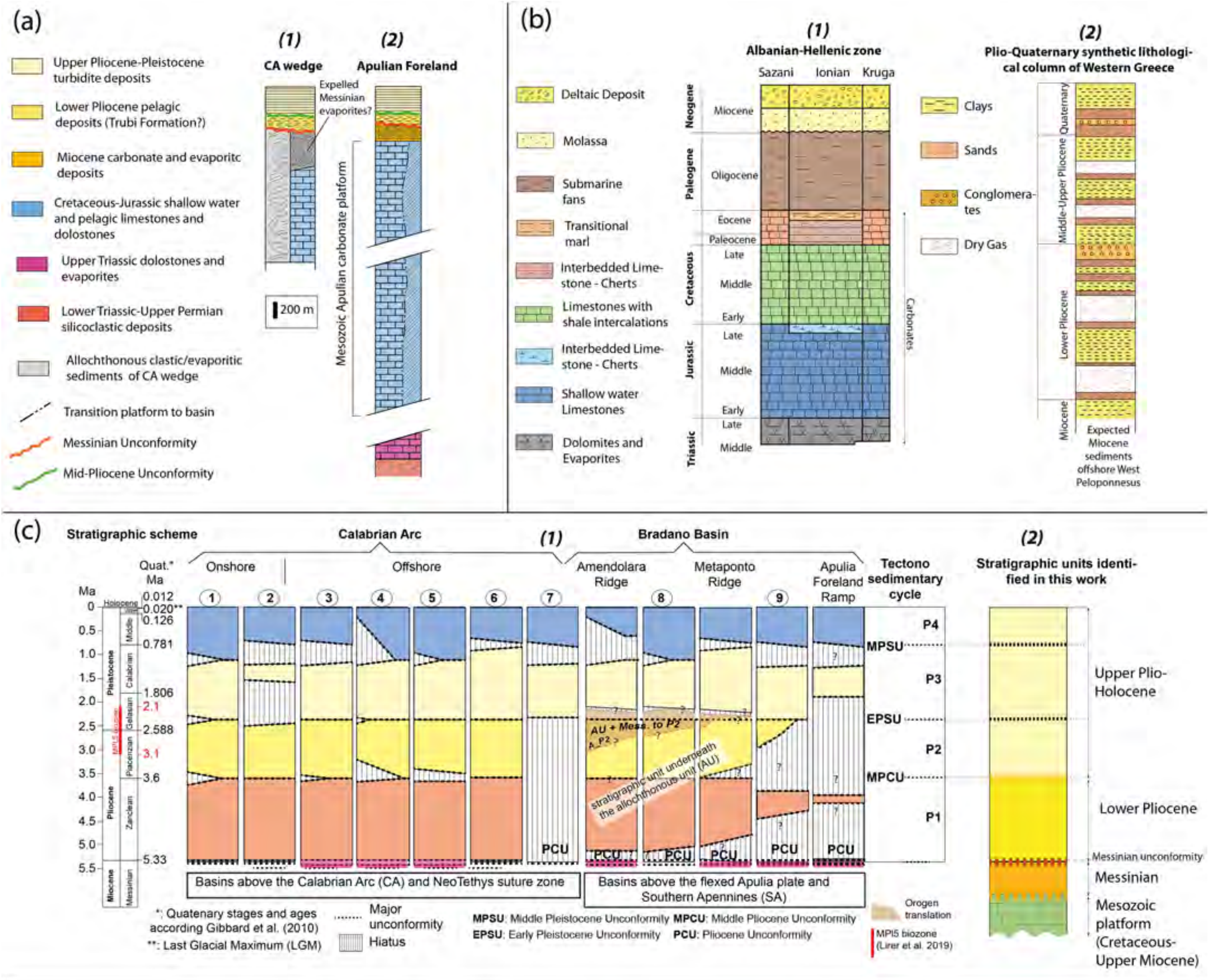
(a)
(1) CA wedge
(2) Apulian Foreland
Upper Pliocene-Pleistocene turbidite deposits
Lower Pliocene pelagic deposits (Trubi Formation?)
Miocene carbonate and evaporitc deposits
Cretaceous-Jurassic shallow water and pelagic limestones and dolostones
Upper Triassic dolostones and evaporites
Lower Triassic-Upper Permian silicoclastic deposits
Allochthonous clastic/evaporitic sediments of CA wedge
Transition platform to basin
Messinian Unconformity
Mid-Pliocene Unconformity
Expelled Messinian evaporites?
200 m
Mesozoic Apulian carbonate platform
(b)
(1) Albanian-Hellenic zone
Sazani
Ionian
Kruga
Deltaic Deposit
Molassa
Submarine fans
Transitional marl
Interbedded Lime-stone - Cherts
Limestones with shale intercalations
Interbedded Lime-stone - Cherts
Shallow water Limestones
Dolomites and Evaporites
Neogene
Miocene
Paleogene
Oligocene
Eocene
Paleocene
Cretaceous
Late
Middle
Early
Jurassic
Late
Middle
Early
Triassic
Late
Middle
Carbonates
(2) Plio-Quaternary synthetic lithological column of Western Greece
Clays
Sands
Conglomera-tes
Dry Gas
Quaternary
Middle-Upper Pliocene
Lower Pliocene
Miocene
Expected Miocene sediments offshore West Peloponnesus
(c)
Stratigraphic scheme
Calabrian Arc
(1)
Bradano Basin
(2)
Onshore
Offshore
Amendolara Ridge
Metaponto Ridge
Apulia Foreland Ramp
Tectono sedimentary cycle
Stratigraphic units identified in this work
Ma
Quat.* Ma
0.012
0.020**
0.126
0.781
1.806
2.1
2.588
3.1
3.6
5.33
Holocene
Pleistocene
Pliocene
Miocene
Calabrian
Gelasian
Piacenzian
Zanclean
Messinian
P4
MPSU
P3
EPSU
P2
MPCU
P1
PCU
AU + Mess. to P2
stratigraphic unit underneath the allochthonous unit (AU)
Upper Plio-Holocene
Lower Pliocene
Messinian unconformity
Messinian
Mesozoic platform (Cretaceous-Upper Miocene)
Basins above the Calabrian Arc (CA) and NeoTethys suture zone
Basins above the flexed Apulia plate and Southern Apennines (SA)
*: Quaternary stages and ages according Gibbard et al. (2010)
**: Last Glacial Maximum (LGM)
Major unconformity
Hiatus
MPSU: Middle Pleistocene Unconformity
MPCU: Middle Pliocene Unconformity
EPSU: Early Pleistocene Unconformity
PCU: Pliocene Unconformity
Orogen translation
MPl5 biozone (Lirer et al. 2019)

Figure 3

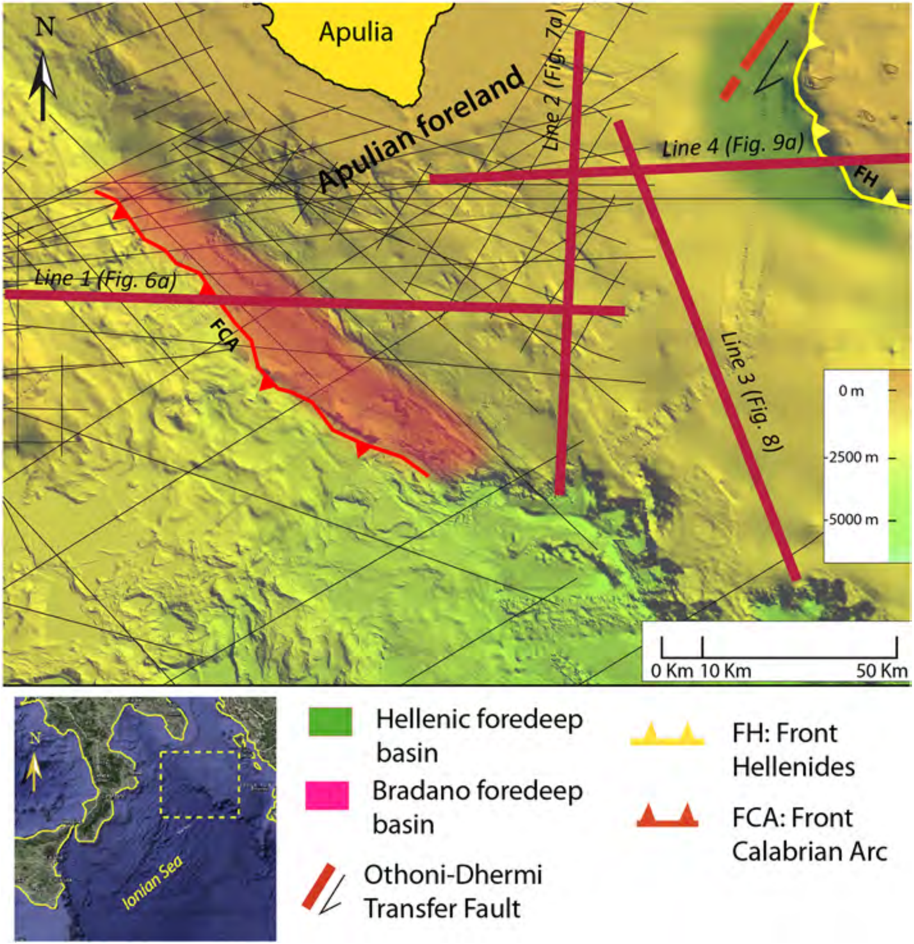

N
Apulia
Apulian foreland
Line 2 (Fig. 7a)
Line 4 (Fig. 9a)
FH
Line 1 (Fig. 6a)
FCA
Line 3 (Fig. 8)
0 m
-2500 m
-5000 m
0 Km 10 Km 50 Km
N
Ionian Sea
Hellenic foredeep basin
Bradano foredeep basin
Othoni-Dhermi Transfer Fault
FH: Front Hellenides
FCA: Front Calabrian Arc

Figure 4

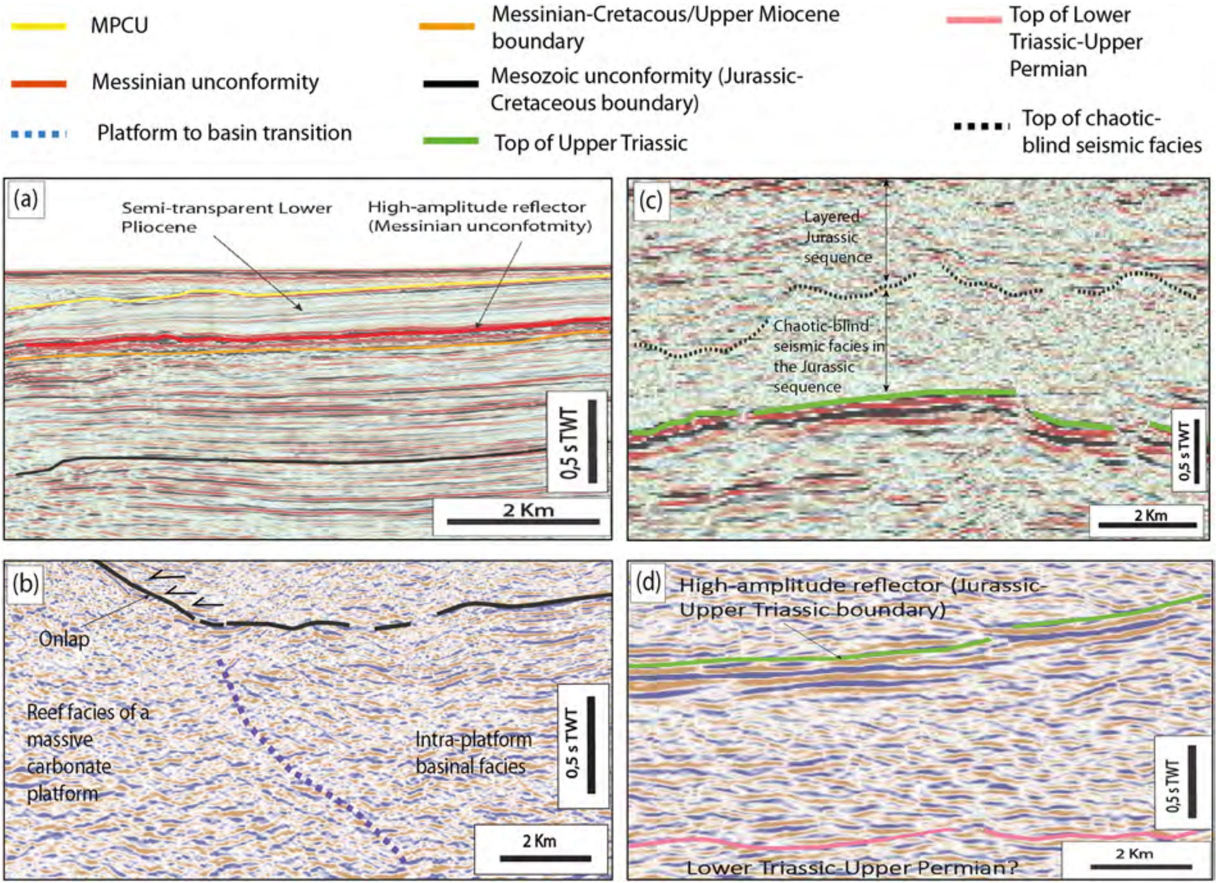
MPCU
Messinian unconformity
Platform to basin transition
Messinian-Cretacous/Upper Miocene boundary
Mesozoic unconformity (Jurassic-Cretaceous boundary)
Top of Upper Triassic
Top of Lower Triassic-Upper Permian
Top of chaotic-blind seismic facies
(a)
Semi-transparent Lower Pliocene
High-amplitude reflector (Messinian unconfotmity)
0,5 s TWT
2 Km
(c)
Layered Jurassic sequence
Chaotic-blind seismic facies in the Jurassic sequence
0,5 s TWT
2 Km
(b)
Onlap
Reef facies of a massive carbonate platform
Intra-platform basinal facies
0,5 s TWT
2 Km
(d)
High-amplitude reflector (Jurassic-Upper Triassic boundary)
0,5 s TWT
2 Km
Lower Triassic-Upper Permian?

Figure 5

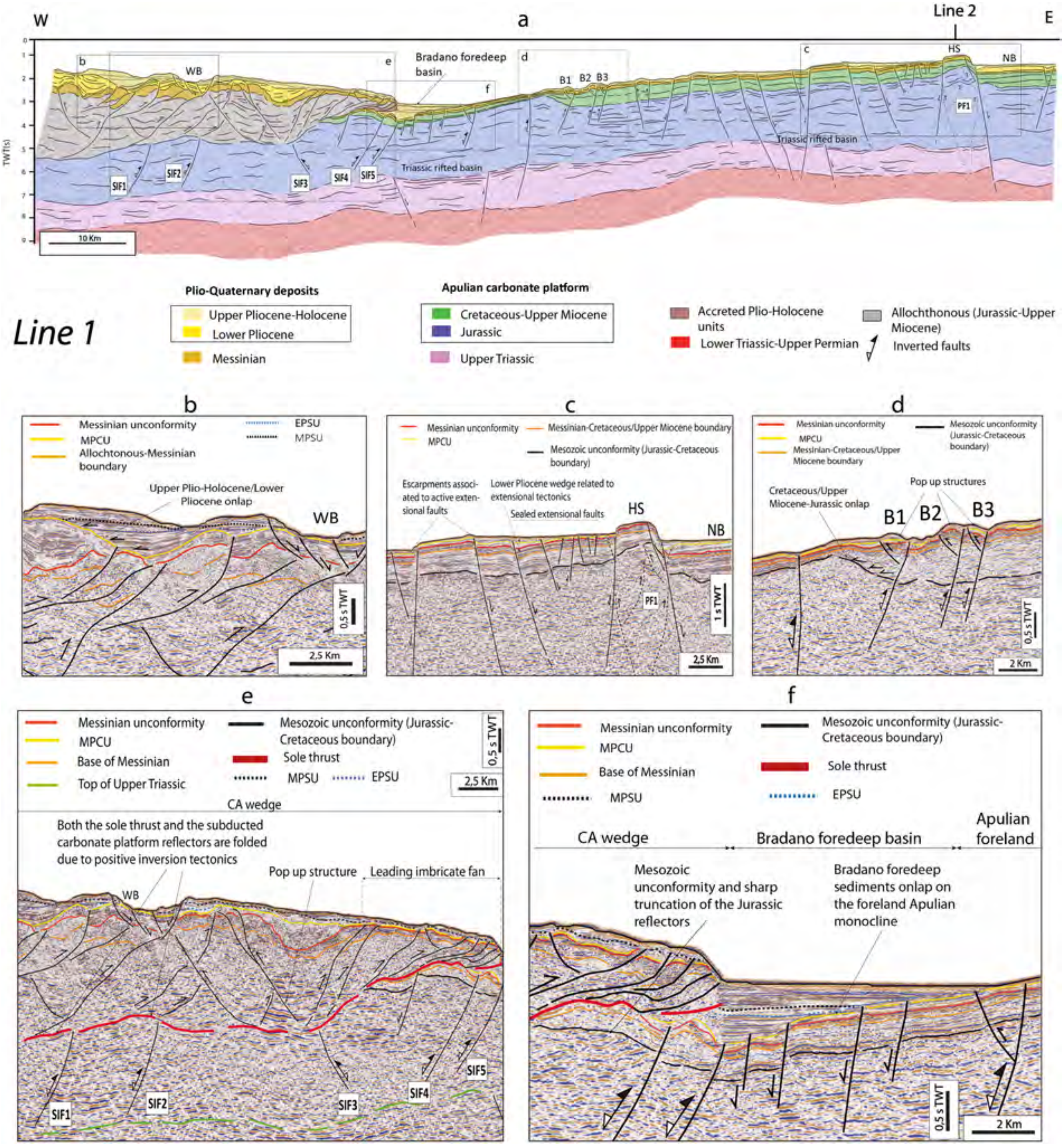

W
a
Line 2
E
HS
NB
Bradano foredeep basin
B1 B2 B3
WB
PF1
Triassic rifted basin
SIF1 SIF2 SIF3 SIF4 SIF5
10 Km
TWT(s)
Plio-Quaternary deposits
Upper Pliocene-Holocene
Lower Pliocene
Messinian
Apulian carbonate platform
Cretaceous-Upper Miocene
Jurassic
Upper Triassic
Accreted Plio-Holocene units
Lower Triassic-Upper Permian
Allochthonous (Jurassic-Upper Miocene)
Inverted faults
Line 1
b
Messinian unconformity
MPCU
Allochtonous-Messinian boundary
EPSU
MPSU
Upper Plio-Holocene/Lower Pliocene onlap
0,5 s TWT
2,5 Km
c
Messinian-Cretaceous/Upper Miocene boundary
Mesozoic unconformity (Jurassic-Cretaceous boundary)
Escarpments associated to active extensional faults
Lower Pliocene wedge related to extensional tectonics
Sealed extensional faults
1 s TWT
d
Messinian-Cretaceous/Upper Miocene boundary
Cretaceous/Upper Miocene-Jurassic onlap
Pop up structures
2 Km
e
Base of Messinian
Top of Upper Triassic
Sole thrust
CA wedge
Both the sole thrust and the subducted carbonate platform reflectors are folded due to positive inversion tectonics
Pop up structure
Leading imbricate fan
f
Apulian foreland
Mesozoic unconformity and sharp truncation of the Jurassic reflectors
Bradano foredeep sediments onlap on the foreland Apulian monocline

Figure 6

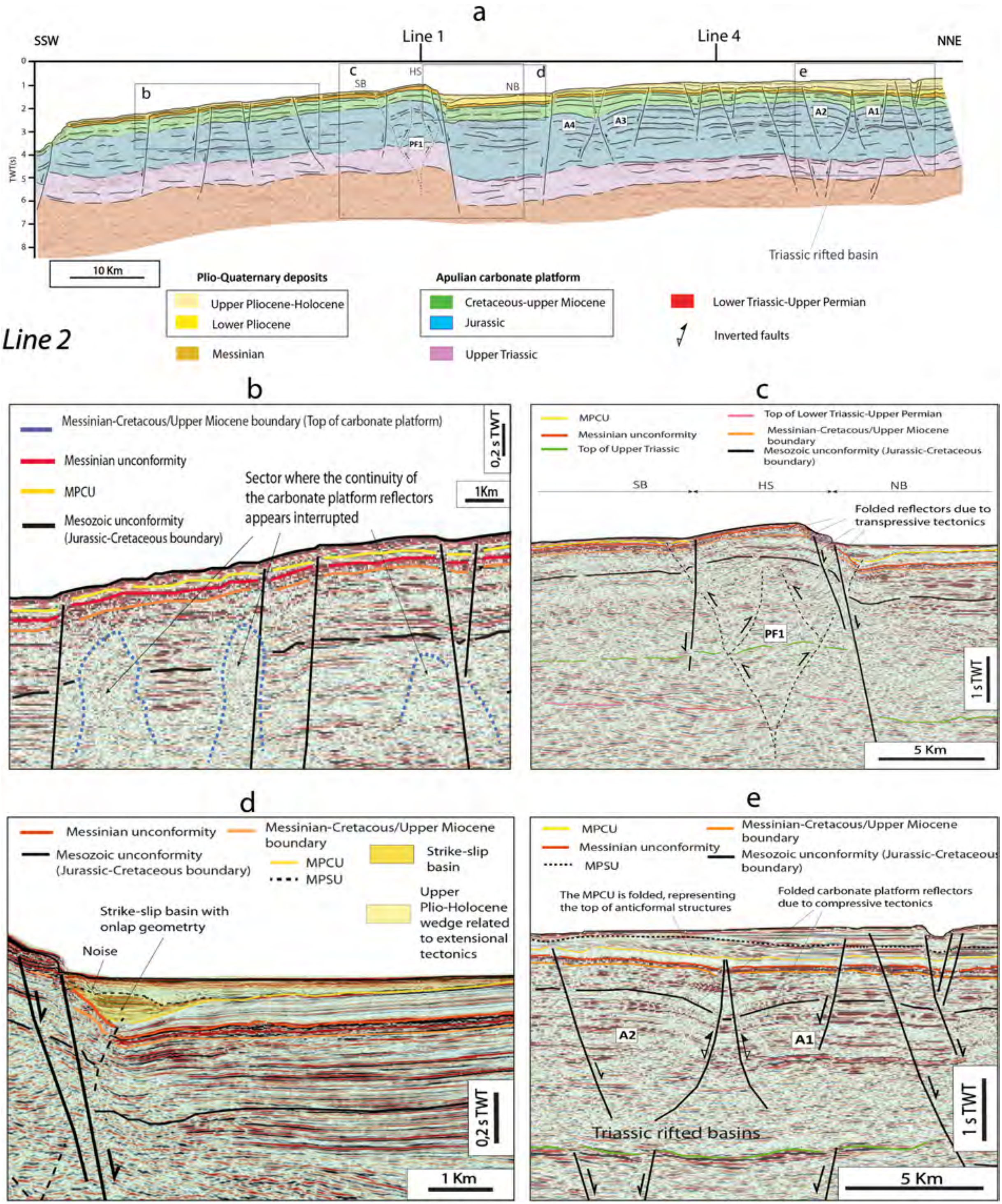
a
SSW
Line 1
Line 4
NNE
TWT(s)
SB
HS
NB
PF1
A4
A3
A2
A1
Triassic rifted basin
10 Km
Plio-Quaternary deposits
Upper Pliocene-Holocene
Lower Pliocene
Messinian
Apulian carbonate platform
Cretaceous-upper Miocene
Jurassic
Upper Triassic
Lower Triassic-Upper Permian
Inverted faults
Line 2
b
Messinian-Cretacous/Upper Miocene boundary (Top of carbonate platform)
Messinian unconformity
MPCU
Mesozoic unconformity (Jurassic-Cretaceous boundary)
Sector where the continuity of the carbonate platform reflectors appears interrupted
0,2 s TWT
1Km
c
MPCU
Messinian unconformity
Top of Upper Triassic
Top of Lower Triassic-Upper Permian
Messinian-Cretacous/Upper Miocene boundary
Mesozoic unconformity (Jurassic-Cretaceous boundary)
SB
HS
NB
Folded reflectors due to transpressive tectonics
PF1
1 s TWT
5 Km
d
Messinian unconformity
Mesozoic unconformity (Jurassic-Cretaceous boundary)
Messinian-Cretacous/Upper Miocene boundary
MPCU
MPSU
Strike-slip basin
Upper Plio-Holocene wedge related to extensional tectonics
Strike-slip basin with onlap geometrty
Noise
0,2 s TWT
1 Km
e
MPCU
Messinian unconformity
MPSU
Messinian-Cretacous/Upper Miocene boundary
Mesozoic unconformity (Jurassic-Cretaceous boundary)
The MPCU is folded, representing the top of anticformal structures
Folded carbonate platform reflectors due to compressive tectonics
A2
A1
Triassic rifted basins
1 s TWT
5 Km

Figure 7

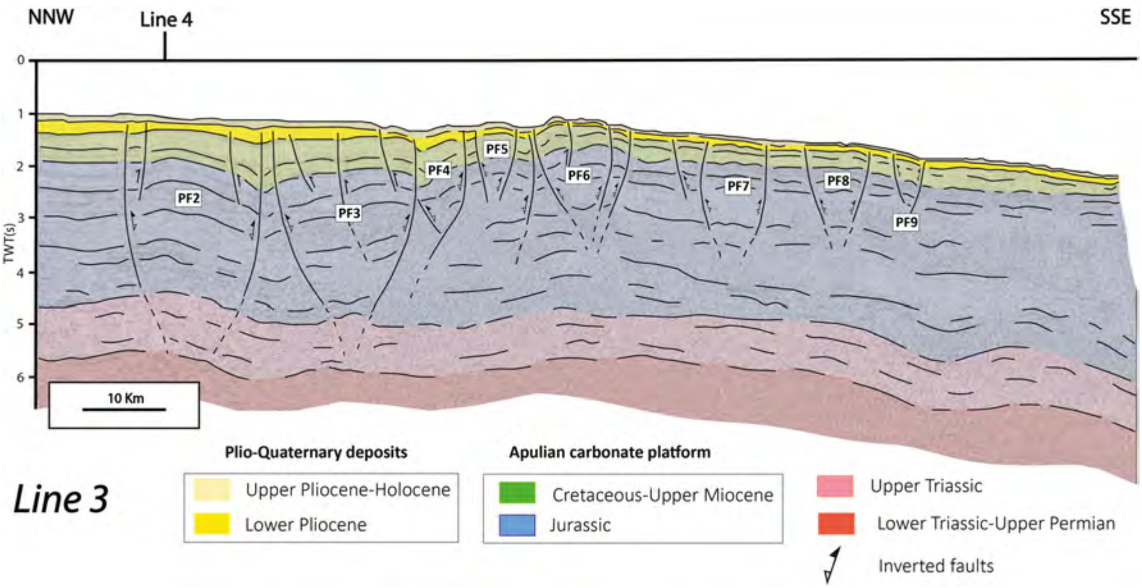
NNW
Line 4
SSE
0
1
2
3
4
5
6
TWT(s)
PF2
PF3
PF4
PF5
PF6
PF7
PF8
PF9
10 Km
Line 3
Plio-Quaternary deposits
Upper Pliocene-Holocene
Lower Pliocene
Apulian carbonate platform
Cretaceous-Upper Miocene
Jurassic
Upper Triassic
Lower Triassic-Upper Permian
Inverted faults

Figure 8

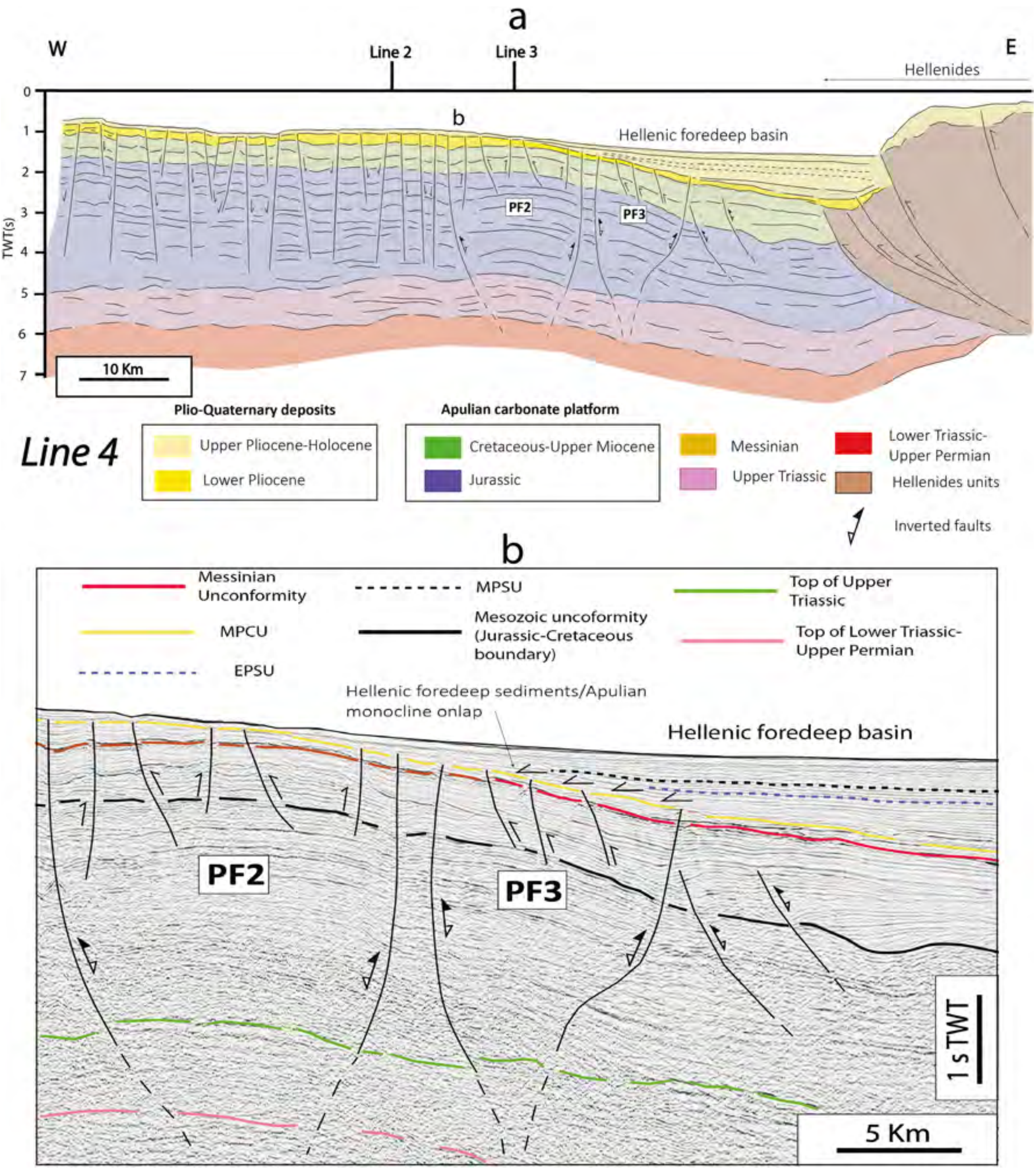

a
W
Line 2
Line 3
E
Hellenides
TWT(s)
0
1
2
3
4
5
6
7
b
Hellenic foredeep basin
PF2
PF3
10 Km
Line 4
Plio-Quaternary deposits
Upper Pliocene-Holocene
Lower Pliocene
Apulian carbonate platform
Cretaceous-Upper Miocene
Jurassic
Messinian
Upper Triassic
Lower Triassic-Upper Permian
Hellenides units
Inverted faults
b
Messinian Unconformity
MPCU
EPSU
MPSU
Mesozoic uncoformity (Jurassic-Cretaceous boundary)
Top of Upper Triassic
Top of Lower Triassic-Upper Permian
Hellenic foredeep sediments/Apulian monocline onlap
Hellenic foredeep basin
PF2
PF3
1 s TWT
5 Km

Figure 9

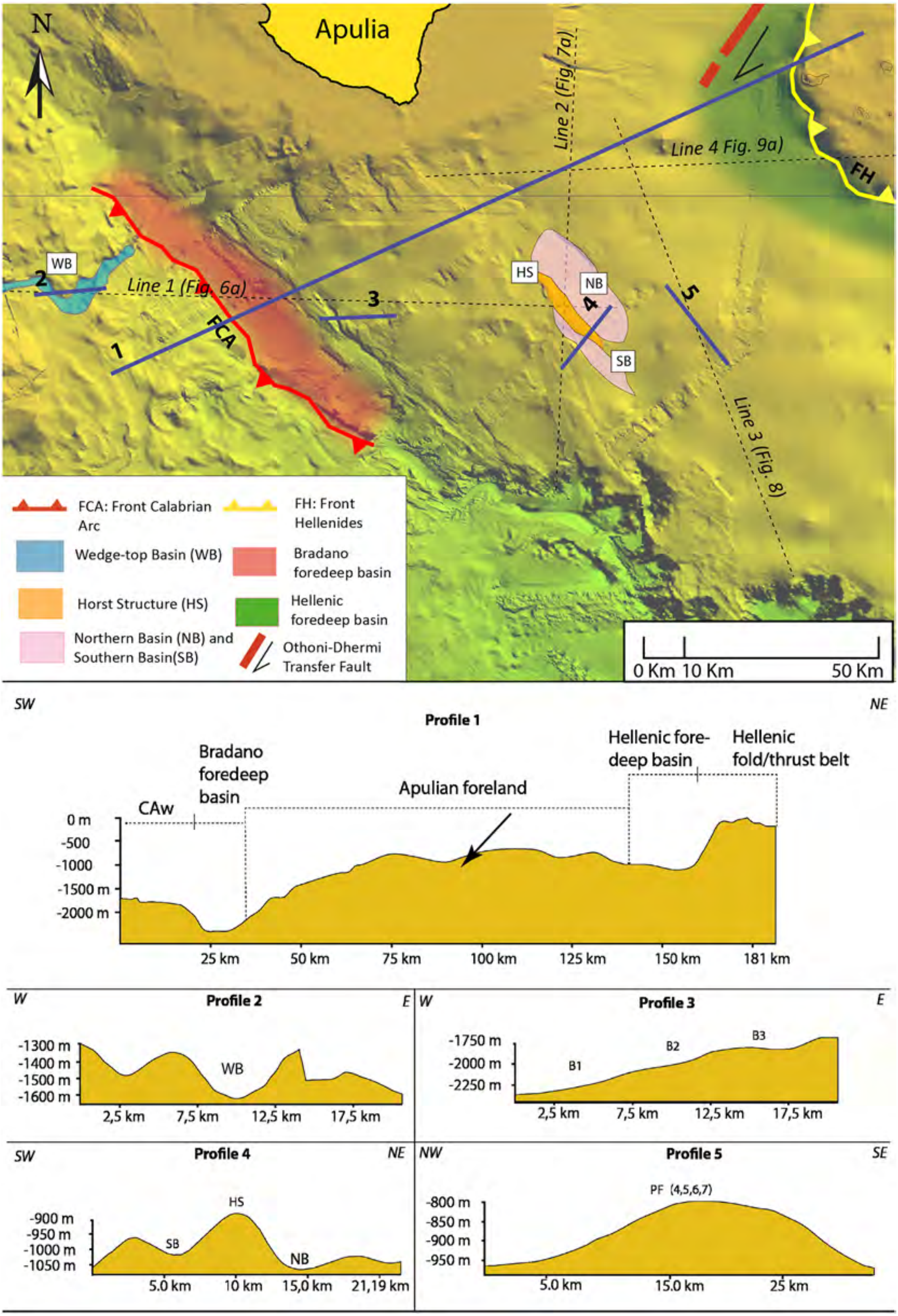
Apulia
N
Line 2 (Fig. 7a)
Line 4 Fig. 9a)
FH
WB
2
Line 1 (Fig. 6a)
3
FCA
1
HS
NB
4
SB
5
Line 3 (Fig. 8)
FCA: Front Calabrian Arc
FH: Front Hellenides
Wedge-top Basin (WB)
Bradano foredeep basin
Horst Structure (HS)
Hellenic foredeep basin
Northern Basin (NB) and Southern Basin(SB)
Othoni-Dhermi Transfer Fault
0 Km 10 Km 50 Km
SW
NE
Profile 1
Bradano foredeep basin
CAw
Apulian foreland
Hellenic fore-deep basin
Hellenic fold/thrust belt
0 m
-500
-1000
-1500 m
-2000 m
25 km
50 km
75 km
100 km
125 km
150 km
181 km
W
E
Profile 2
-1300 m
-1400 m
-1500 m
-1600 m
WB
2,5 km
7,5 km
12,5 km
17,5 km
W
E
Profile 3
-1750 m
-2000 m
-2250 m
B1
B2
B3
2,5 km
7,5 km
12,5 km
17,5 km
SW
NE
Profile 4
-900 m
-950 m
-1000 m
-1050 m
HS
SB
NB
5.0 km
10 km
15,0 km
21,19 km
NW
SE
Profile 5
-800 m
-850 m
-900 m
-950 m
PF (4,5,6,7)
5.0 km
15.0 km
25 km

Figure 10

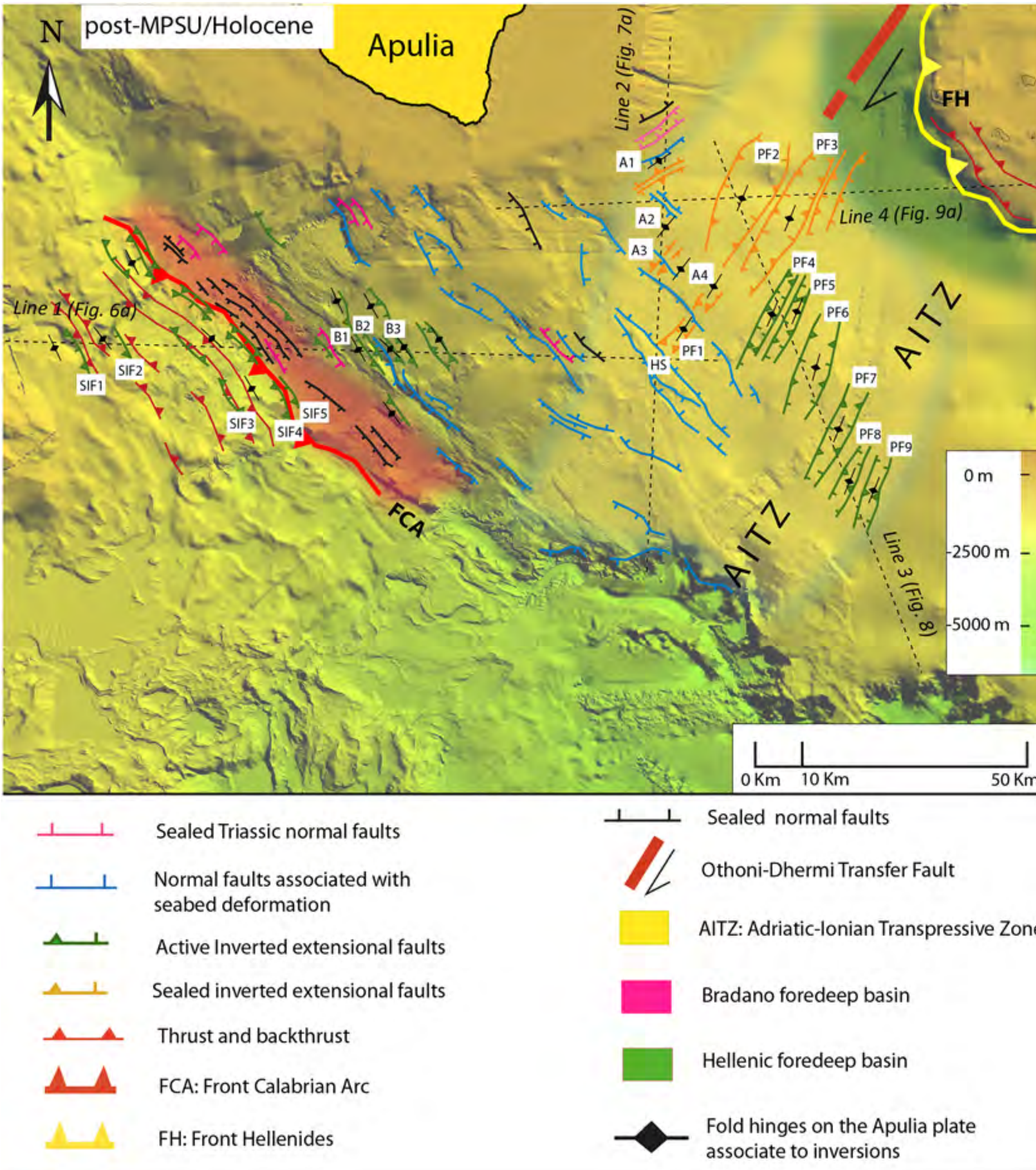
post-MPSU/Holocene
N
Apulia
FH
Line 2 (Fig. 7a)
Line 4 (Fig. 9a)
Line 1 (Fig. 6a)
Line 3 (Fig. 8)
A1
A2
A3
A4
PF1
PF2
PF3
PF4
PF5
PF6
PF7
PF8
PF9
B1
B2
B3
HS
SIF1
SIF2
SIF3
SIF4
SIF5
FCA
AITZ
AITZ
0 m
-2500 m
-5000 m
0 Km
10 Km
50 Km
Sealed Triassic normal faults
Normal faults associated with seabed deformation
Active Inverted extensional faults
Sealed inverted extensional faults
Thrust and backthrust
FCA: Front Calabrian Arc
FH: Front Hellenides
Sealed normal faults
Othoni-Dhermi Transfer Fault
AITZ: Adriatic-Ionian Transpressive Zone
Bradano foredeep basin
Hellenic foredeep basin
Fold hinges on the Apulia plate associate to inversions

Figure 11

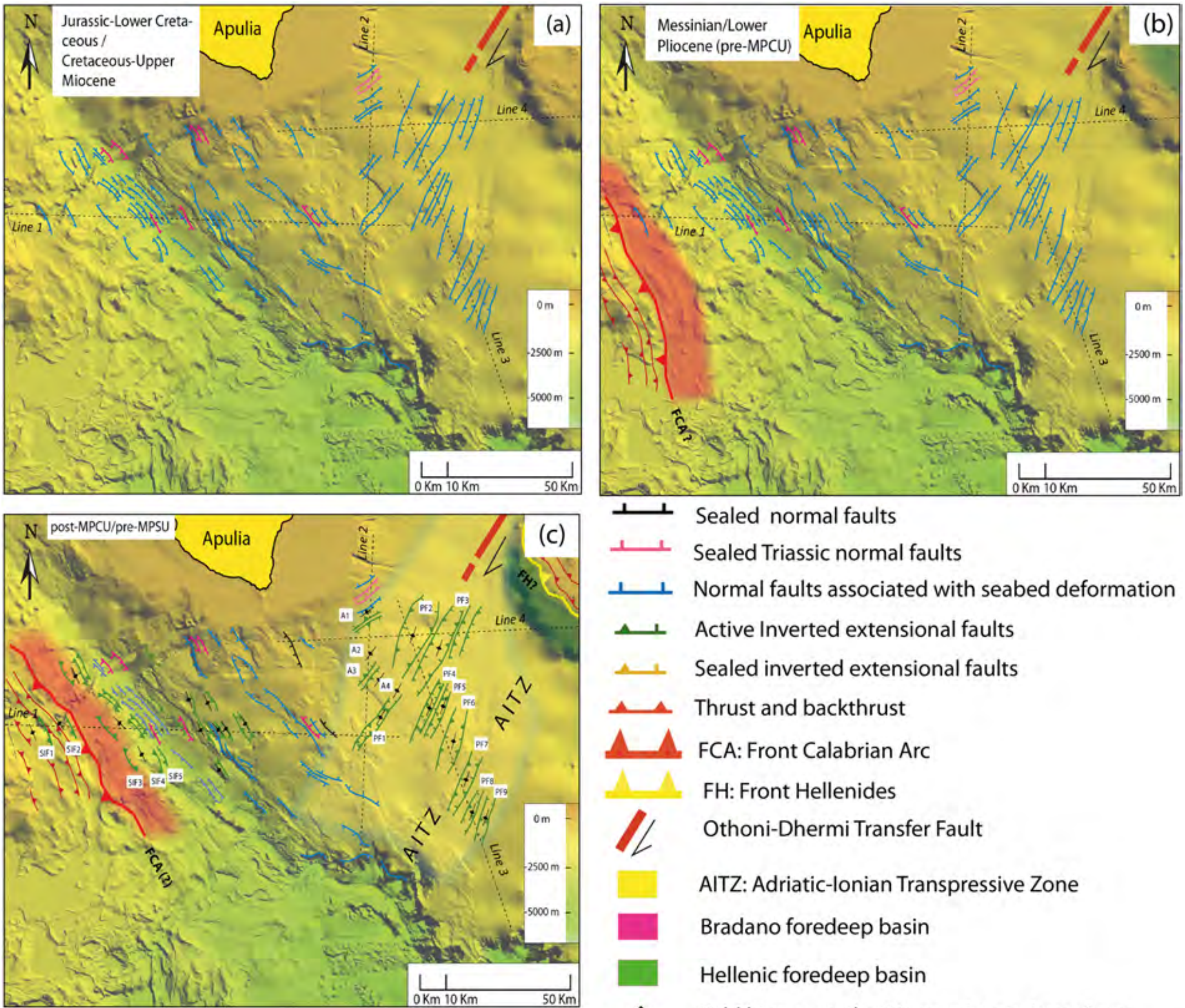

(a)
Jurassic-Lower Cretaceous / Cretaceous-Upper Miocene
Apulia
Line 1
Line 2
Line 3
Line 4
0 m
-2500 m
-5000 m
0 Km 10 Km 50 Km
(b)
Messinian/Lower Pliocene (pre-MPCU)
Apulia
FCA ?
(c)
post-MPCU/pre-MPSU
Apulia
FH?
AITZ
FCA (?)
A1
A2
A3
A4
PF1
PF2
PF3
PF4
PF5
PF6
PF7
PF8
PF9
SIF1
SIF2
SIF3
SIF4
SIF5
Sealed normal faults
Sealed Triassic normal faults
Normal faults associated with seabed deformation
Active Inverted extensional faults
Sealed inverted extensional faults
Thrust and backthrust
FCA: Front Calabrian Arc
FH: Front Hellenides
Othoni-Dhermi Transfer Fault
AITZ: Adriatic-Ionian Transpressive Zone
Bradano foredeep basin
Hellenic foredeep basin
Fold hinges on the AP associate to inversions

Figure 12

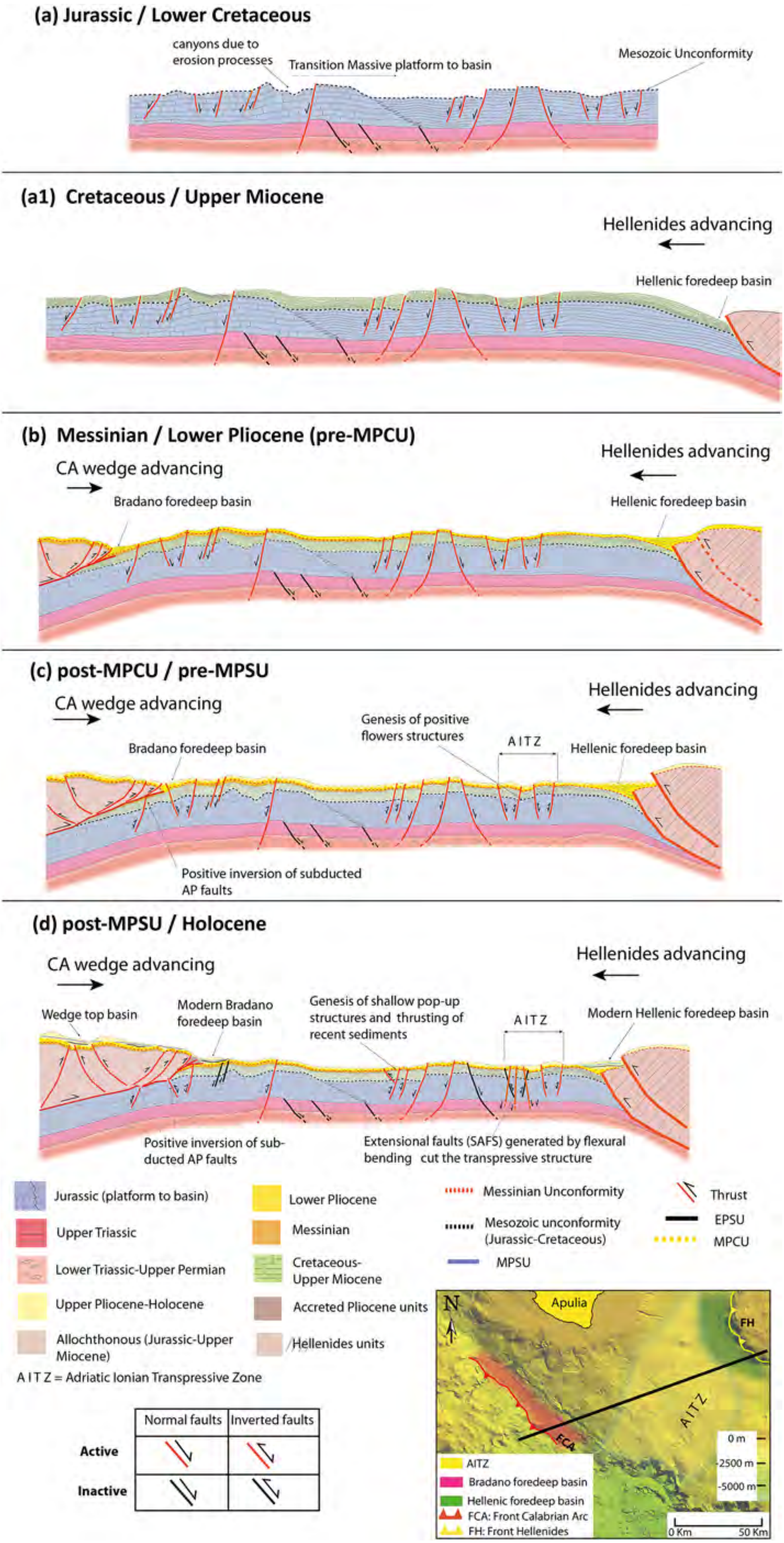
(a) Jurassic / Lower Cretaceous
canyons due to erosion processes
Transition Massive platform to basin
Mesozoic Unconformity
(a1) Cretaceous / Upper Miocene
Hellenides advancing
Hellenic foredeep basin
(b) Messinian / Lower Pliocene (pre-MPCU)
CA wedge advancing
Bradano foredeep basin
Hellenides advancing
Hellenic foredeep basin
(c) post-MPCU / pre-MPSU
CA wedge advancing
Bradano foredeep basin
Genesis of positive flowers structures
A I T Z
Hellenides advancing
Hellenic foredeep basin
Positive inversion of subducted AP faults
(d) post-MPSU / Holocene
CA wedge advancing
Wedge top basin
Modern Bradano foredeep basin
Genesis of shallow pop-up structures and thrusting of recent sediments
A I T Z
Hellenides advancing
Modern Hellenic foredeep basin
Positive inversion of sub-ducted AP faults
Extensional faults (SAFS) generated by flexural bending cut the transpressive structure
Jurassic (platform to basin)
Upper Triassic
Lower Triassic-Upper Permian
Upper Pliocene-Holocene
Allochthonous (Jurassic-Upper Miocene)
A I T Z = Adriatic Ionian Transpressive Zone
Lower Pliocene
Messinian
Cretaceous-Upper Miocene
Accreted Pliocene units
Hellenides units
Messinian Unconformity
Mesozoic unconformity (Jurassic-Cretaceous)
MPSU
Thrust
EPSU
MPCU
Normal faults
Inverted faults
Active
Inactive
N
Apulia
FH
AITZ
FCA
0 m
-2500 m
-5000 m
AITZ
Bradano foredeep basin
Hellenic foredeep basin
FCA: Front Calabrian Arc
FH: Front Hellenides
0 Km
50 Km

Figure 13

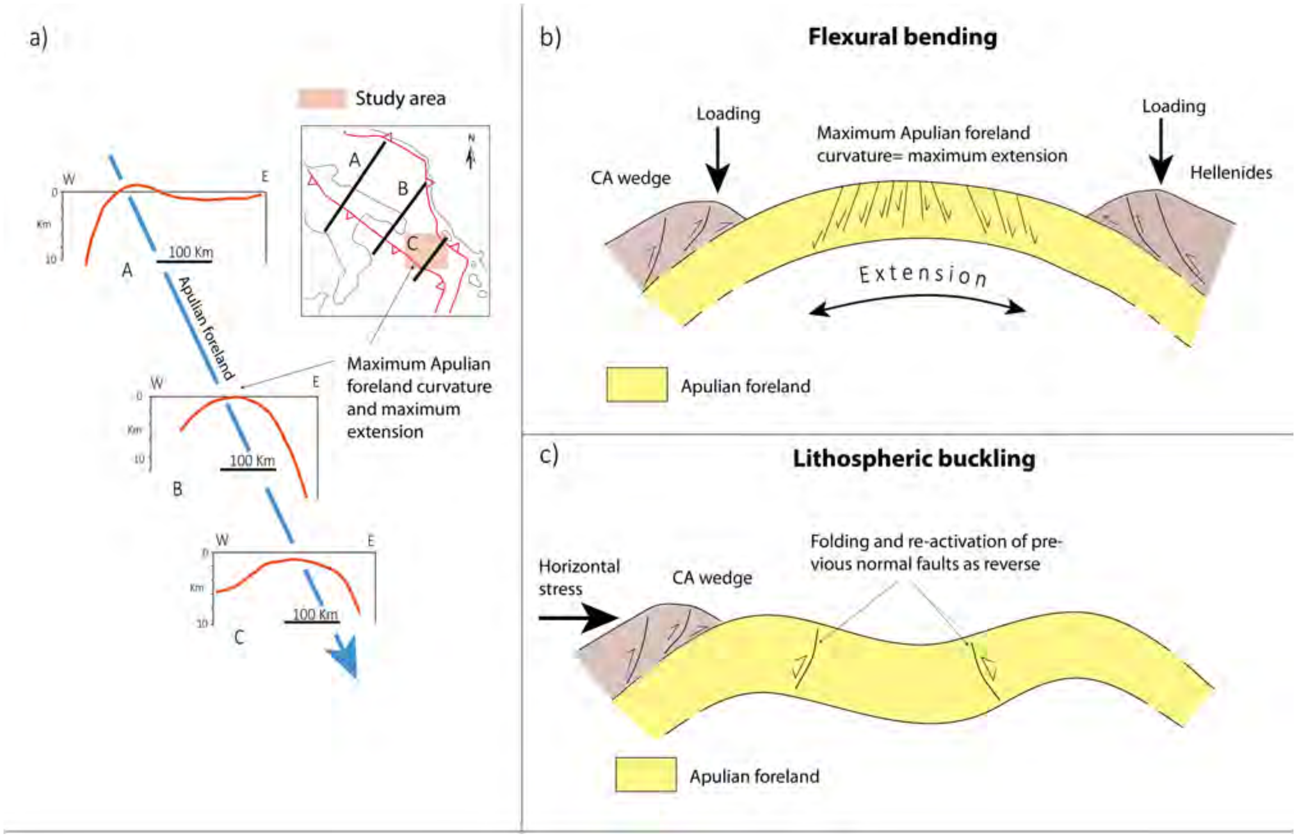
a)
Study area
A
B
C
W
E
0
Km
10
100 Km
Apulian foreland
Maximum Apulian foreland curvature and maximum extension
b)
Flexural bending
Loading
Maximum Apulian foreland curvature= maximum extension
Loading
CA wedge
Hellenides
Extension
Apulian foreland
c)
Lithospheric buckling
Folding and re-activation of previous normal faults as reverse
Horizontal stress
CA wedge
Apulian foreland

Figure 14

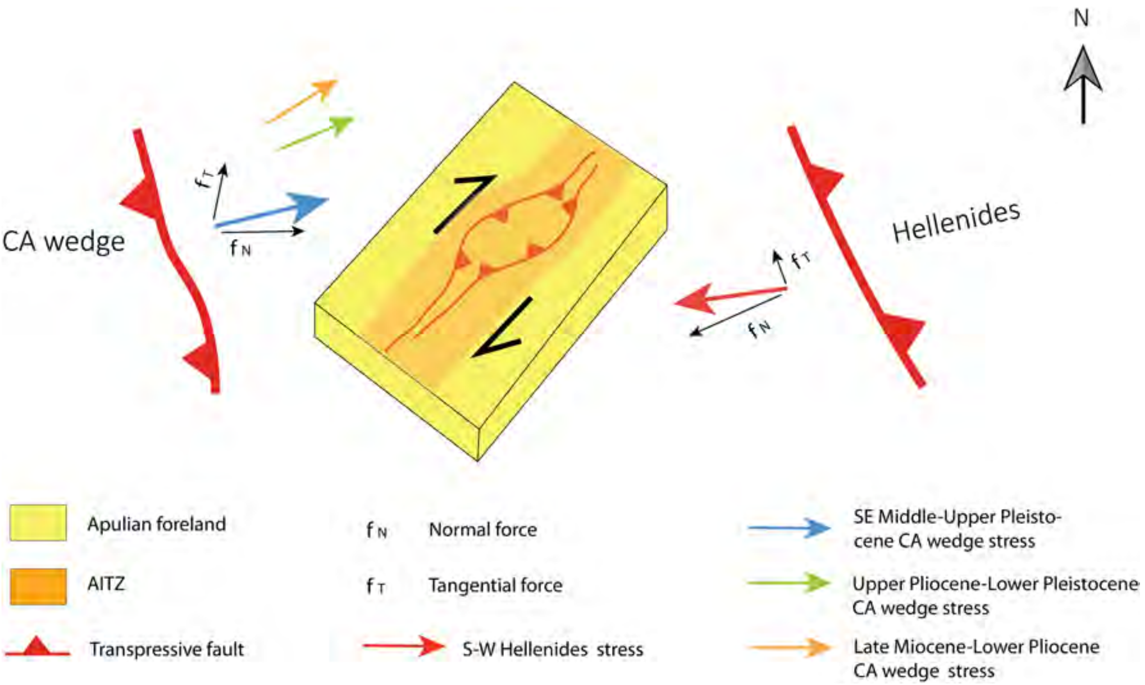
N
CA wedge
Hellenides
f T
f N
f T
f N
Apulian foreland
AITZ
Transpressive fault
f N Normal force
f T Tangential force
S-W Hellenides stress
SE Middle-Upper Pleistocene CA wedge stress
Upper Pliocene-Lower Pleistocene CA wedge stress
Late Miocene-Lower Pliocene CA wedge stress

Figure 15